

Accelerated flooding along the U. S. East Coast: On the impact of sea level rise, tides, storms, the Gulf Stream and NAO

Tal Ezer and Larry P. Atkinson

Center for Coastal Physical Oceanography , Old Dominion University
Corresponding author: T. Ezer (tezer@odu.edu)

Revision submitted to “**Earth’s Future**”: July 7, 2014

1 **Abstract.**

2
3 Recent studies identified the U.S. East Coast north of Cape Hatteras as a “hotspot” for accelerated sea
4 level rise (SLR), and the analysis presented here show that the area is also a “hotspot for accelerated
5 flooding”. The duration of minor tidal flooding (defined as 0.3 m above MHHW) has accelerated in
6 recent years for most coastal locations from the Gulf of Maine to Florida. The average increase in annual
7 minor flooding duration was ~20 hours from the period until 1970 to 1971-1990, and ~50 hours from
8 1971-1990 to 1991-2013; spatial variations in acceleration of flooding resembles the spatial variations of
9 acceleration in sea level. The increase in minor flooding can be predicted from SLR and tidal range, but
10 the frequency of extreme storm-surge flooding events (0.9 m above MHHW) is less predictable, and
11 affected by the North Atlantic Oscillations (NAO). The number of extreme storm surge events since
12 1960 oscillates with a period of ~15-year and interannual variations in the number of storms is anti-
13 correlated with the NAO index. With higher seas, there are also more flooding events that are unrelated
14 to storm surges. For example, it is demonstrated that week-long flooding events in Norfolk, VA, are
15 often related to periods of decrease in the Florida Current transport. The results indicate that previously
16 reported connections between decadal variations in the Gulf Stream and coastal sea level may also apply
17 to short-term variations, so flood predictions may be improved if the Gulf Stream influence is
18 considered.

19 1. Introduction

20 High relative sea level rise (SLR) rates recorded by tide gauges along the U.S. East Coast (Fig.
21 1) and sea level acceleration north of Cape Hatteras, North Carolina [Boon, 2012; Ezer and Corlett,
22 2012; Sallenger et al., 2012; Kopp, 2013; Ezer, 2013; Ezer et al., 2013] are expected to increase coastal
23 flooding associated with tides and storm surges. The Mid-Atlantic coastal region has been called a “hot
24 spot of accelerated SLR”, and positive acceleration has been calculated by at least 4 different statistical
25 methods [Boon, 2012; Ezer and Corlett, 2012; Sallenger et al., 2012; Kopp, 2013]. However, how to
26 detect statistically significant sea level acceleration is still being debated [Haigh et al., 2014], and
27 uncertainties remain about the implications of sea level acceleration for the likelihood of future flooding
28 and coastal risk management issues [Nicholls and Cazenave, 2010; Cazenave and Cozannet, 2014].
29 Therefore, we will show here that acceleration in flooding extent is more clearly detectable than
30 acceleration in SLR rates; both accelerations are correlated with each other and show similar spatial
31 patterns along the coast. Moreover, flooding statistics, as presented in this study, are useful for practical
32 purposes of developing flood mitigation strategies. Several low-lying populated regions along the U. S.
33 coasts are especially vulnerable to SLR, including south Florida [Zhang, 2011], and the Hampton Roads
34 region in the lower Chesapeake Bay [Kleinosky et al., 2007; Atkinson et al., 2013; Boesch et al., 2013;
35 Mitchell et al., 2013]. In addition to large land subsidence around the Chesapeake Bay area due to
36 Glacial Isostatic Adjustment, GIA [Boon et al., 2010; Kopp, 2013], SLR acceleration in the Mid-
37 Atlantic coastal region has been found to be highly correlated with recent offshore shift and weakening
38 in the Gulf Stream just north of Cape Hatteras, as seen in altimeter data [Ezer et al., 2013] and in direct
39 observations of the Florida Current [Ezer, 2013]. The latter finding is consistent with dynamic sea level
40 changes seen in ocean models [Ezer, 1999, 2001, Levermann et al., 2005; Yin et al., 2009; Yin and
41 Goddard, 2013] and expected weakening in the Atlantic Meridional Overturning Circulation (AMOC)
42 under warmer climate conditions [Hakkinen and Rhines, 2004; Sallenger et al., 2012; McCarthy et al.,
43 2012; Srokosz et al., 2012; Smeed et al., 2013]. Although the long-term weakening of the GS is still
44 small and difficult to detect [Rossby et al., 2013], variations on scales ranging from weeks to decades
45 may result in large temporal and spatial variations of SLR rates along the U.S. East Coast [Kopp, 2013;
46 Ezer, 2013].

47 The motivation for our study comes from the fact that temporal and spatial variations in sea level
48 pose challenging questions on how to assess the flooding risk of coastal regions. For example, it is well
49 recognized that a storm surge larger than normal may occur if a hurricane landfall coincides with high
50 tide (e.g., when storm Sandy hit New Jersey and New York in 2012), but less understood is the
51 possibility that a storm surge coincides with a period of relatively higher sea level due to seasonal
52 variations or a weaker GS [Sweet et al., 2009]. Periods of anomalous high water can last weeks or
53 months [Sweet et al., 2009], and possibly years or decades [Ezer et al., 2013; Ezer, 2013]. There are
54 numerous studies that assess the risk of extreme events, for example, Kemp and Horton [2013] study the
55 contribution of SLR and high tide timing to hurricane flooding in New York City over the past ~200
56 years, while Zhang and Sheng [2013] used observations and numerical model simulations to study the
57 contribution of storms and tides to extreme sea level events along the eastern coast of North America.
58 The latter study did not consider the impact of SLR, and neither study considered the impact of changes
59 in ocean dynamics or the GS. For each tide gauge in the U.S. NOAA provides statistics of 1%, 10%,
60 50%, and 99% annual exceedance probability (tidesandcurrents.noaa.gov). For example, 1%
61 exceedance probability means that the likelihood of water level reaching particular water level in any
62 year is in average 1/100; an extreme storm surge event of this type is “the average recurrence interval”
63 [see Hunter, 2010 for definitions]. But how to interpret such information or use it for risk management
64 or mitigation planning is not always clear. Moreover, the NOAA exceedance statistics is based on the

65 average of past measurements, so it does not consider how the likelihood of flooding has changed in the
 66 past and how it will change in the future due to the impact of SLR. A simple statistical method to
 67 estimate the expected exceedance under future SLR has been offered by *Hunter* [2012]. However, in the
 68 study presented here we do not attempt to calculate probability statistics of sea level, as it has already
 69 been done by other studies mentioned above. Instead, we provide more practical information on the
 70 duration of (potential) flooding when water level reached a particular level and how the likelihood of
 71 floods change over time and space. Moreover, while most other studies focus on extreme storm surge
 72 events, we also provide flood statistics for minor and moderate tidal flooding events which are not
 73 catastrophic, but very important for people living near waterfronts and coasts. Such information was
 74 found to be very useful to communicate flood risks to the local population and planners in the flood-
 75 prone region around the city of Norfolk, VA [*Atkinson et al.*, 2013] and along the shores of the
 76 Chesapeake Bay [*Boesch et al.*, 2013; *Mitchell et al.*, 2013].

77 Observed coastal relative sea level at a particular time (t) and location (x) is the result of several
 78 components,

$$79 \quad h(x, t) = DAT(x) + GLB(t) + SUB(x, t) + LOC(x, t) + TID(x, t) + STO(x, t). \quad (1)$$

81 Each component have different temporal (T) and spatial (X) scales: DAT is a reference datum (the
 82 current National Tidal Datum Epoch is based on averages for 1983-2001), GLB is the global SLR (T~
 83 decades to centuries), SUB is the local land subsidence due to GIA (X~ 100-1000 km; T~1000s of
 84 years), LOC is local changes due to groundwater extraction, weather pattern, ocean dynamics, changes
 85 in gravity field due to mass redistribution and other processes not homogeneous in space (X~ 10s-100s
 86 km; T~ days to years), TID is the tidal contribution (T~ hours-days) and STO is major storm surge
 87 events (T~ months-years). For short term sea level variations, GLB, SUB and TID contributions are the
 88 most predictable and the LOC and STO the most unpredictable.

89 Fig. 2 shows an example of the different contributions to a high-water storm event in Norfolk,
 90 where the local SLR is ~1.5 times larger than the altimeter derived global mean sea level of the past ~20
 91 years and ~3 times larger than the tide-gauge derived [*Church and White*, 2011] global mean SLR of the
 92 past century. In the past, GIA was responsible to the large local SLR in Norfolk [*Boon et al.*, 2010], but
 93 additional acceleration in SLR in recent years may be due to weakening GS since ~2004 according to
 94 *Ezer et al.* [2013], so one needs to assess the impact on these changes in ocean currents on potential
 95 flooding. We define a storm surge event as a period when water level reached a particular level above
 96 Mean High-High Water (MHHW). For example, Fig. 3 shows that 17 extreme storm surge events
 97 occurred in Norfolk over the past 85 years, when water level reached at least 0.9 m (~3 feet) above
 98 MHHW. The impact of SLR is also demonstrated in Fig. 3- the top storm surge was caused by the
 99 Chesapeake-Potomac Hurricane of 1933 when sea level was ~0.4 m lower than today, so a storm surge
 100 with similar strength if occurring today could cause water level to reach ~2 m above MHHW. Note also
 101 that, more than half of the big storm surges occurred during the past 15 years, but only one storm
 102 occurred in a 35-year span, between 1963-1997 suggesting that SLR as well as decadal variations may
 103 affect the frequency of storm events. The changing frequency of storm events will thus be addressed in
 104 this study. However, the frequency of storm events and the maximum water level reached for each storm
 105 do not accurately represent the flooding risk and damage. For example, the most flooding in Norfolk
 106 happened during the “Veterans Day Northeast” of 2009 because floods lasted for several tidal cycles
 107 when water continued to flow into more streets compared with much stronger hurricanes when water
 108 receded immediately after the storm passed. To capture this phenomenon, from hourly sea level data,
 109

110 $h(t)$, the total hours of flooding per year (T) for each station (“ i ”) are calculated for 3 selected critical
111 water levels (WLC above MHHW),
112

113
$$T_i^{year} = \sum_{year} t \quad ; \quad h(t) > WLC, \quad WLC = 0.3, \quad 0.6, \quad 0.9m \quad . \quad (2)$$

114
115 Note that local topography and coastal slopes may result in a non-linear relation between SLR and actual
116 inundation [Zhang, 2011], so a more detailed analysis is needed to determine if a particular place will be
117 flooded or not. However, the 3 categories of flooding defined by WLC roughly represent (for example in
118 downtown Norfolk) minor tidal flooding (that is sometimes referred to as “nuisance flooding” with wet
119 streets), moderate weather related flooding (e.g., a weather front passing during Spring tide) and extreme
120 storm events (e.g., a hurricane or major nor’easter), respectively. Note that the calculations based on Eq.
121 2 are directly related to the exceedance probability and the average recurrence interval [e.g., see Hunter,
122 2010, for definitions]; the higher the critical water level WLC , the lower the recurrence interval is.
123 However since exceedance probability is routinely calculated by NOAA, it is not repeated here. Instead,
124 analyzing how flooding frequency and duration change between different locations and how they are
125 affected by the different components in Eq. 1, as well as by large scale Atlantic Ocean variations, are the
126 main goals of this study.

127

128 2. Sea level data

129 Hourly sea level records from 11 tide gauge stations were obtained from NOAA
130 (<http://opendap.co-ops.nos.noaa.gov/dods/>). The locations are shown in Fig. 1 and information on each
131 station, including tidal range and SLR, are listed in Table 1. The data cover 4 different regions along the
132 U. S. coast, 3 stations in the Gulf of Maine, 3 stations in the Mid-Atlantic Bight, 3 stations in the South
133 Atlantic Bight and one station (Key West) between the Florida Strait and the Gulf of Mexico (Fig. 1).
134 Only stations with relatively long and continuous hourly records were used, with an average period of
135 87 years. These stations represent large variations in tidal range, from ~0.5 m (the southernmost point,
136 Key West, FL) to ~6 m (the northernmost point, Eastport, ME). With these data, the impact of tidal
137 range on flooding can be evaluated. The mean (relative) SLR rate varies from ~1.9 mm y^{-1} (Gulf of
138 Maine) to ~4-5 mm y^{-1} (lower Mid-Atlantic Bight). Note that most studies of SLR use monthly data,
139 which may cover in some stations longer records than the hourly data, so the SLR rates in Table 1 are
140 slightly different than those reported by Ezer [2013], Boon [2012] and others. Ezer [2013] described the
141 significant spatial difference in mean SLR and acceleration between stations north and south of Cape
142 Hatteras, apparently a dynamic response related to the separation point of the Gulf Stream from the
143 coast. However, the spatial pattern of flooding along the coast may be more complex, since in addition
144 to the spatial pattern of SLR, variations in tidal range and in the frequency of storms also vary along the
145 coast, as quantified recently by Zhang and Sheng [2013].

146

147 3. Results

148 3.1. Flood duration and frequency: impact of sea level rise and tides

149 Communities prone to flooding often prepare for flood events based on expected water level
150 (relative to say MHHW) obtained from tide and storm surge models. For example, in a flood-prone
151 neighborhood near downtown Norfolk, high tide is sometimes accompanied by unexplained anomalous
152 high waters that may reach 0.3m (~1foot) above MHHW even when there is no local wind events (see
153 more on this in section 3.3). This condition can result in minor tidal flooding that can cause what is
154 referred to as “nuisance flooding”. When an additional weather front passes the region during high tide,

155 water level may reach 0.6m (~2feet) above MHHW and more streets will be flooded. During a major
156 tropical storm, nor'easter or hurricane, water level could reach over 0.9m (~3feet) above MHHW (Fig.
157 3) and several blocks of city streets from the water front will be completely under water. In the later case
158 flood gates in the downtown area of the city and in highway tunnels would be closed. Therefore, the
159 same statistics of annual flooding time that has been used to characterize floods and plan mitigation
160 strategies in Norfolk [Atkinson *et al.*, 2013] have been extended here to other locations; examples are
161 shown in Fig. 4a-4g and the results for all the 11 locations are listed in Table 1. Note that the terms
162 "minor", "moderate" and "major" flooding events refer here to 0.3, 0.6 and 0.9 m above MHHW,
163 though specific locations may have different coastal slopes, height of streets above water or some
164 protection measures (e.g., flood walls), so that the actual flood risk may be different.

165 The impact of tidal range on potential flooding can be seen for example in the difference
166 between Eastport (Fig. 4a) and Portland (Fig. 4b). The two stations located in the same region, the Gulf
167 of Maine, have similar tidal modulation (Neap/Spring tide relation) and similar SLR, but the tidal range
168 is almost twice as large in Eastport than it is in Portland (Table 1), resulting in 2-10 times longer flood
169 duration in Eastport than that in Portland. Note that tidal range by itself may not predict the exceedance
170 probability very well if tidal modulation is different, as demonstrated for example by some Australian
171 stations [Hunter, 2012]. The potential for minor, moderate or major floods in Eastport are dominated by
172 the high tide, and between 1958 and 2009 the increase in flooding due to SLR is relatively small.
173 However, in every year since 2010 major floods (top panel of Fig. 4a) are larger than in any year before
174 2010. This may relate to the unusual warming north of the Gulf Stream that started around 2004 and
175 affected the lobster fishery in the Gulf of Main [Mills *et al.*, 2013]. In Portland (Fig. 4b) and Boston (not
176 shown) on the other hand, significant increase in minor and moderate flooding due to SLR is more
177 visible, but extreme sea level ("major flooding") is rare and shows only decadal variations with no
178 apparent gradual increase. In the Mid-Atlantic region, New York (Fig. 4c), Atlantic City and Lewes (not
179 shown) and Norfolk (Fig. 4d), dramatic increase in minor and moderate flooding is seen, which is
180 consistent with the high SLR and recent acceleration of SLR in this region [Boon, 2012; Sallenger *et al.*,
181 2012; Kopp, 2013; Ezer, 2013; Ezer *et al.*, 2013]. In Norfolk, for example (Fig. 4d), years with more
182 than 50 hours of minor flooding were very rare until the 1980s (4 times in over 50 years) and only
183 happened when nor'easters or hurricanes passed the region. However, over the past 20 years, minor
184 flooding of 50-250 hours per year became commonplace. In the South Atlantic Bight, the pattern of
185 flooding is quite different than that of the Mid-Atlantic region, since relative coastal SLR associated
186 with land subsidence (term SUB in Eq. 1) is not as large, and SLR acceleration is smaller than that in the
187 Mid-Atlantic coastal region [Boon, 2012; Ezer, 2013]. In Wilmington there seem to be a significant
188 increase in minor flooding after the 1980s but it is attributed to an increase in tidal range (bottom panel
189 of Fig. 4e) and not due to SLR alone. The tidal station is located in the Cape Fear River; the river has
190 seen continuous sediment filling and several cycles of dredging over the years, which apparently
191 changed the tidal dynamics. In Wilmington (Fig. 4e) and Charleston (Fig. 4f), major floods are rare and
192 happened only during a couple of hurricanes. Key West, with its small tidal range (Fig. 4g), experienced
193 an increase in minor flooding only over the past decade, and almost no major floods except a single
194 year, 2005 (when hurricanes Katrina and Wilma passed nearby).

195 Fig. 5 summarizes the minor flooding (0.3 m above MHHW) hours at the 11 locations; the
196 averaged annual flooding is calculated for three periods: 1. Before 1971, 2. 1971-1990, and 3. 1991-
197 2013. While all stations show significant increase in flooding from the 1970s to the 1990s and 2000s, an
198 apparent spatial pattern emerges from this comparison. Three locations are clearly distinct from the
199 general pattern: the northernmost location, Eastport, has such a large tidal range that it is the only
200 location with high minor floods (over 40 hours) even before 1971, while the southernmost point, Key

201 West, has very minimal floods throughout the record. Wilmington, just south of Cape Hatteras, also has
 202 an unusual pattern, with almost no flooding until 1990, but a large increase of 10 fold in recent years due
 203 to local sand fill and dredging that caused an increased tidal range, as discussed before. There is a
 204 significant increase in flooding at all locations, which is typically ~200% to 600% after the 1990s
 205 relative to the floods experienced before the 1970s. The question is- “Is there a consistent acceleration in
 206 flooding?” The acceleration in minor flooding is estimated by
 207

$$208 \quad ACC(hr / yr^2) = \frac{\frac{(T3 - T2)}{(Y3 - Y2)} - \frac{(T2 - T1)}{(Y2 - Y1)}}{(Y3 - Y1) / 2} \quad (3)$$

209
 210 Y1, Y2 and Y3 are the years in the middle of the 3 periods, from the beginning of the record to 1970,
 211 from 1971 to 1990 and from 1991 to 2013, respectively, and T1, T2 and T3 are the average annual
 212 flooding hours for the 3 periods. All the stations show positive acceleration (Table 1), and a distinct
 213 pattern. Excluding the northernmost and southernmost stations, acceleration in flooding increases
 214 gradually as one moves south from Portland (ACC~0.01 hr yr²) to Lewes and Norfolk (ACC~0.15 hr
 215 yr²), and then from Wilmington (ACC~0.04 hr yr²) to Pulaski (ACC~0.08 hr yr²). The change in the
 216 acceleration at Cape Hatteras and the general pattern of ACC closely resembles the SLR acceleration
 217 pattern found by *Ezer* [2013]. Although acceleration in SLR is not necessarily precondition for
 218 acceleration in flooding, the similarity in the pattern of spatial variations between acceleration in SLR
 219 and flooding suggests that ocean dynamics (i.e., term LOC in Eq. 1) may play a role in causing the
 220 differences between the Mid-Atlantic Bight north of Cape Hatteras and the South Atlantic Bight south of
 221 Cape Hatteras. Fig. 6 compares the acceleration in minor flooding (ACC) with the acceleration in sea
 222 level, calculated by *Ezer* [2013]; the latter uses an Empirical Mode Decomposition (EMD) method to
 223 separate a non-linear trend from oscillating modes [see *Ezer and Corlett*, 2012, for details]. Data at
 224 Eastport was omitted in Fig. 6 due to its unusual high tide that obscures the results. Results show that
 225 accelerations in sea level and in floods are significantly correlated (R=0.77, confidence level>99%). The
 226 largest acceleration in both, sea level and flood duration is at Norfolk, VA, and Lewes, DE, the closest
 227 locations downstream from the separation point of the Gulf Stream at Cape Hatteras. The locations with
 228 the lowest flood acceleration are those farthest away from Cape Hatteras in both directions (Portland in
 229 the north and Key West in the south).

230 The contributions of tides and SLR to (minor) flooding are shown in Fig. 7 (excluding data from
 231 Wilmington due to varying tidal range). Before 1990, flooding period was highly correlated with the
 232 tidal range (correlation coefficient R>0.9 and statistical confidence >99.9%) and only small differences
 233 are seen between the period before 1971 and 1971-1990. After 1990 SLR seems to play an additional
 234 role, so the correlation between tidal range and flooding is somewhat smaller (R=0.77, though still
 235 significant at 99% level). The fact that all 3 lines in Fig. 6a have almost the same slope indicates that
 236 tidal contribution to flooding is quite linear and predictable. The average increase in minor flooding is
 237 ~20 hours per year between the beginning of the records to 1970 and 1971-1990, but ~50 hours per year
 238 between 1971-1990 and 1991-2013.

239
 240 **3.2. Extreme sea level events and the impact of the North Atlantic Oscillations**

241 Extreme storm surge events (defined here at 0.9 m over MHHW) are relatively rare and are
 242 related to hurricanes or intense storms (except where tides are very large, such as in Eastport). A storm
 243 such as Hurricane Sandy caused more floods in 2012 than a storm with similar strength 100 years ago
 244 when sea level was lower (assuming both hit at the same tidal stage) [*Kemp and Horton*, 2013].

245 However, predicting the frequency of big storms and the location they hit the coast may be difficult and
246 depend on many factors, such as variations of weather and climate over the continental U.S. and
247 conditions over the Atlantic Ocean. Fig. 3 and Fig. 4 (and the other stations not shown) indicate that
248 extreme sea level events in the Mid-Atlantic region have some decadal-like variations rather than a
249 gradual increase as seen in minor and moderate flooding events, suggesting a modulation by large-scale
250 ocean-atmosphere patterns.

251 One of the most widely used patterns that affect decadal and multidecadal variations in the
252 Atlantic region is the North Atlantic Oscillation (NAO) index [Hurrell, 1995], representing north-south
253 dipole of pressure anomalies over the North Atlantic Ocean. The NAO is associated with changes in the
254 intensity and location of the jet stream and storm track, as well as changes in temperature and
255 precipitation patterns. For example, strong positive phases of the NAO tend to be associated with
256 warmer temperatures in the eastern U. S. The NAO may also be connected to long-term variations in sea
257 level and the transport of the GS [Ezer *et al.*, 2013]. An extreme storm surge event is defined here as a
258 year with at least one event with water level reaching at least 0.9 m above MHHW (i.e., a non-zero bar
259 in the upper panels of Fig. 4). While it is possible that a single storm moving along the coast may cause
260 extreme events at more than one location, they are considered here as separate events, since we attempt
261 to characterize the total impact of storms on the coast. An index of the average number per year of
262 extreme storm events hitting somewhere along the coast for each 5-year period is shown in Fig. 8 (green
263 line) and compared with 5-year averages of the NAO index (blue line). Note that only stations with at
264 least 2 extreme events were included. The small number of events do not allow calculating statistical
265 significance, but qualitatively there seem to be interesting relations between NAO and extreme events.
266 The average number of extreme storm surge events per year generally increased from ~0.5 before 1950
267 to ~3.5 in 1990; at the same time the NAO shows an upward trend as well; Hurrell [1985] and others
268 described this multidecadal shift in the NAO. An increase in storminess [Dowson *et al.*, 2002] and
269 warmer temperatures along the U.S. coast associated with more positive NAO [Mills *et al.*, 2013] may
270 relate to this trend, though more research on this possibility is needed, which is beyond the scope of this
271 study. During the time between the 1970s and 1990s the sub-polar region also experienced an increase
272 in sea level and weakening circulation [Hakkinen and Rhines, 2004] which may have weakened the
273 AMOC and the GS transports [Ezer *et al.*, 2013]. An interesting result is that between 1950 and 2010
274 there is an oscillation in the number of extreme events with a period of about 15 years (significant peaks
275 in extreme events in 1960-1965, 1975-1980, 1990-1995 and 2005-2010). Those variations show that
276 minima and maxima and extreme events are anti-correlates with peaks in the NAO (7 such cases are
277 indicated by the vertical red bars in Fig. 8), so more storms seem to be expected during a period when
278 NAO reached a local minimum. These variations could relate to wind-driven decadal variations in the
279 Atlantic Ocean circulation and GS transport (which was found to be anti-correlated with NAO
280 variations; Ezer *et al.*, 2013). In any case, while SLR contributes to the damage caused by extreme storm
281 surge events, it does not seem to explain the decadal pattern of extreme flooding events, so one needs to
282 consider also large-scale atmosphere-ocean patterns.

283

284 **3.3. Minor short term flooding and the impact of the Gulf Stream**

285 Recent studies suggest a strong connection between long-term variations in the GS and coastal
286 sea level [Ezer, 2013; Ezer *et al.*, 2013], whereas weakening of the GS reduces the sea level slope across
287 the GS, resulting in lower water level east of the GS and higher water level onshore along the coast. The
288 same studies found that variations in the GS strength, estimated from either satellite altimeter data over
289 the Mid-Atlantic Bight [Ezer *et al.*, 2013], or from direct observations of the Florida Current transport
290 across the Florida Strait [Ezer, 2013], produce similar correlations with decadal variations in coastal sea

291 level. Connections between the GS transport at the Florida Straits and coastal sea level, from Key West
292 to Norfolk, on seasonal time-scales, have been suggested as well [Blaha, 1985]. High-frequency (e.g.,
293 meso-scale or wind-driven) variations in the strength of the GS may also influence high-frequency
294 variations in coastal sea level. For example, a NOAA report [Sweet *et al.*, 2009] suggests that unusually
295 high water level along the mid-Atlantic coast in the summer of 2009 may have been related to a period
296 of weak Florida Current transport. Low-lying cities in the Chesapeake Bay, such as Norfolk, Virginia,
297 noticed in recent years prolong periods of flooding during high tides when water levels exceed the
298 official NOAA prediction by 0.3-0.5 m, even when there is no storm in the region. Wind-driven
299 numerical models seem to underestimate these events by as much as 0.5 m. Could such events be partly
300 responsible for the increased in frequency of minor flooding events as observed around the Chesapeake
301 Bay [Atkinson *et al.*, 2013; Mitchell *et al.*, 2013; Boesch *et al.*, 2013]?. As an example, Fig. 8a shows the
302 hourly tidal prediction and observed water level in Sewells Point, Norfolk, for the first three months of
303 2013. During this period, there were no major storms, but at least 6 events when the observed water
304 level was at least 20 cm above the NOAA prediction for more than one tidal cycle (causing minor street
305 flooding in downtown Norfolk), and one event of extremely low observed water level of 40 cm below
306 the prediction (day 50). While some of the short (~1 day) anomalies may be due to local wind, there is
307 no atmospheric explanation for high water anomaly that lasts for weeks (e.g., days 55-75). When
308 comparing the water level anomaly (or residual) to the daily Florida Current transport [Baringer *et al.*,
309 2013] (Fig. 8b), it was found that the change in the transport is highly anti-correlated ($R=-0.5$;
310 significance >99%) with the water level (Fig. 8c). When the FC (i.e., the GS measured at the Florida
311 Strait) is on a weakening trend such as from February 20 to March 12, water level is considerably higher
312 than normal (with only a short break when the FC increased slightly at day 65). Ezer *et al.* [2013]
313 noticed that on decadal scales water level in the mid-Atlantic coast have higher correlations with
314 changes in the GS (after it separated from the coast), then the correlation with the GS strength itself; a
315 simple dynamic balance equations were presented by Ezer *et al.* to explain this relation. They also show
316 significant correlation on monthly to decadal scales between the FC cable transport upstream of Cape
317 Hatteras and altimeter-derived GS strength downstream of Cape Hatteras. Here it was shown that the
318 same mechanism also works for high-frequency oscillations. The fact that there is no time lag between
319 changes in the Florida Current at 27°N and changes in sea level more than 1000 km farther north,
320 indicates that the entire western boundary current may have some coherent variations that are probably
321 driven by Ekman transports associated with variations in the large-scale wind stress over the subtropical
322 gyre [McCarthy *et al.*, 2012]. A recent study, using data and models, in fact, supports the hypothesis
323 suggested above, it shows coherent correlation between FC transport and sea level along the GS from
324 south Florida to 40°N and coherent correlation between the FC transport and wind stress over the
325 subtropical gyre [Fig. 4 in Zhao and Johns, 2014]. If oceanic anomalies in sea level propagate toward
326 the coast by means of fast moving barotropic waves, the response at the coast would be within hours.
327 More research is needed on this driving mechanism, which is beyond the scope of this paper. However,
328 a practical implication of the finding is the possibility to improve water level prediction on the coast
329 using GS data from either satellite or the Florida Current cable measurements.

330

331 **4. Summary and conclusions**

332 Recent findings show an accelerated SLR (“hotspot”) along the U.S. east coast north of Cape
333 Hatteras and significant variations of SLR rates along the coast [Boon, 2012; Ezer and Corlett, 2012;
334 Sallenger *et al.*, 2012; Kopp, 2013; Ezer, 2013]; a potential driver for those may be climate-related
335 changes in the AMOC [Hakkinen and Rhines, 2004; McCarthy *et al.*, 2012; Srokosz *et al.*, 2012; Smeed
336 *et al.*, 2013] and its upper branch, the Gulf Stream [Ezer *et al.*, 2013]. But it is not always clear how this

337 information can be used to assess risks and impacts on different coasts and cities vulnerable to flooding
338 [Nicholls and Cazenave, 2010; Cazenave and Cozannet, 2014]. Therefore, we calculated here a matrix
339 of flood statistics, based on 3 given water level above a known high tide reference level (representing
340 “minor”, “moderate” and “extreme” flood events); this analysis is more easily used for practical
341 purposes of flood mitigation and risk assessment than standard exceedance probability statistics (though
342 the two methods are related). The results show very clearly that the U. S. East Coast (in particular the
343 Mid-Atlantic coastal area north of Cape Hatteras) is a “hotspot of accelerated flooding” and that
344 acceleration in SLR is highly correlated with acceleration in minor flood durations. Minor to moderate
345 flooding increased significantly in the 1990s. Until the 1980s, the increase in flooding was relatively
346 moderate, and flooding was, in most cases, associated with particular storm events. However, in recent
347 years, flooding became more common and even a small weather front or anomaly related to offshore
348 currents change can cause flooding over several tidal cycles. The result is acceleration in flooding
349 durations, with larger increase in flooding along the coasts of the lower Mid-Atlantic Bight, where SLR
350 acceleration is also larger. An interesting result was that extreme storm surge events seem to be
351 correlated with decadal and multi-decadal variations of the NAO, in addition to the general increase in
352 flooding due to SLR. It was found that decadal oscillations (of ~15 year period) in the number of
353 extreme storm surge events are anti-correlated with decadal variations in the NAO; the results are
354 consistent with mechanism involved wind-driven oscillations in the Atlantic Ocean circulation and the
355 Gulf Stream [Ezer, 1999, 2001; Ezer et al., 2013].

356 What are the implications of these results with respect to flood risks due to future SLR? The
357 average recurrence interval is expected to change, so in Norfolk, for example, a flood with a 80-year
358 return level (define by an annual exceedance probability of 1/80) today is expected to occur in average
359 every ~40 years if sea level would rise by 0.1 m; by 2050 when sea level in Norfolk is expected to rise
360 by ~0.5 m [Boon, 2012; Ezer and Corlett, 2012] such flood level will be expected to occur every ~6
361 years (based on our calculations, not shown, and statistics provided by NOAA). The increase in the
362 impact of storm surges due to rising seas and potentially due to slowing down of the Gulf Stream will
363 result in increase in flood durations, as demonstrated here. The main goal of this study was to provide
364 information on flood statistics, spatial variations and the various forcing components involved, in the
365 hope that such information will be useful for improving flood predictions and for planning mitigation
366 and adaptation strategies in flood-prone regions such as the Hampton Roads area (where the authors
367 reside).

368
369 **Acknowledgments:** Old Dominion University’s Climate Change and Sea Level Rise Initiative
370 (CCSLRI) as well the Center for Coastal Physical Oceanography (CCPO) provided partial support for
371 this study. John Hunter and an anonymous reviewer are thanked for providing many useful suggestions
372 that greatly improved the paper. Access to all the hourly tide gauge data is available from
373 <http://opendap.co-ops.nos.noaa.gov/dods/IOOS/> and the Matlab-based codes to plot all figures are
374 available on request from tezer@odu.edu. The NAO index data can be obtained from
375 <http://climatedataguide.ucar.edu>.

376 377 **References**

- 378 Atkinson, L. P., T. Ezer and E. Smith, (2013), Sea level rise and flooding risk in Virginia, *Sea Grant*
379 *Law and Policy Journal*, Vol. 5, No. 2, 3-14.
- 380 Baringer, M. O., W. E. J., G. McCarthy, J. Willis, S. Garzoli, M. Lankhorst, C. S. Meinen, U. Send, W.
381 R. Hobbs, S. A. Cunningham, D. Rayner, D. A. Smeed, T. O. Kanzow, P. Heimbach, E. Frajka-
382 Williams, A. Macdonald, S. Dong, and J. Marotzke (2013), Meridional overturning circulation and

383 heat transport observations in the Atlantic Ocean [in “State of the Climate in 2012”], *Bull. Amer.*
384 *Meteor. Soc.*, 94 (8), S65–S68.

385 Blaha, J. P. (1984), Fluctuations of monthly sea level as related to the intensity of the Gulf Stream from
386 Key West to Norfolk. *J. Geophys. Res. Oceans*, 89(C5), 8033-8042.

387 Boesch, D.F., L.P. Atkinson, W.C. Boicourt, J.D. Boon, D.R. Cahoon, R.A. Dalrymple, T. Ezer, B.P.
388 Horton, Z.P. Johnson, R.E. Kopp, M. Li, R.H. Moss, A. Parris, C.K. Sommerfield, (2013), Updating
389 Maryland's Sea-level Rise Projections, *Special Report of the Scientific and Technical Working Group*
390 *to the Maryland Climate Change Commission*, 22 pp. University of Maryland Center for
391 Environmental Science, Cambridge, MD.

392 Boon, J. D. (2012) Evidence of sea level acceleration at U.S. and Canadian tide stations, Atlantic coast,
393 North America, *J. Coast. Res.*, 28(6), 1437 – 1445, doi:10.2112/JCOASTRES-D-12-00102.1.

394 Boon, J. D., J. M. Brubaker and D. R. Forrest (2010), Chesapeake Bay land subsidence and sea level
395 change, in *App. Mar. Sci. and Ocean Eng., Report No. 425*, Virginia Institute of Marine Science,
396 Gloucester Point, VA.

397 Cazenave, A. and G. L. Cozannet (2014), Sea level rise and its coastal impacts. *Earth's Future*, 2: 15–
398 34. doi: 10.1002/2013EF000188.

399 Church, J. A. and N. J. White (2011), Sea-level rise from the late 19th to the early 21st century, *Surv.*
400 *Geophys.*, 32, 585–602, doi:10.1007/s10712-011-9119-1.

401 Dawson, A. G., K. Hickey, T. Holt, L. Elliott, S. Dawson, I. Foster, P. Wadhams, I. Jonsdottir, J.
402 Wilkinson, J. McKenna, N. R. Davis and D. E. Smith (2002), Complex North Atlantic Oscillation
403 (NAO) index signal of historic North Atlantic storm-track changes. *The Holocene* 12(3), 363-369.

404 Ezer, T. (1999), Decadal variabilities of the upper layers of the subtropical North Atlantic: An ocean
405 model study, *J. Phys. Oceanogr.*, 29(12), 3111-3124.

406 Ezer, T. (2001), Can long-term variability in the Gulf Stream transport be inferred from sea level?,
407 *Geophys. Res. Lett.*, 28(6), 1031-1034.

408 Ezer, T. and W. B. Corlett (2012), Is sea level rise accelerating in the Chesapeake Bay? A demonstration
409 of a novel new approach for analyzing sea level data, *Geophys. Res. Lett.*, 39, L19605,
410 doi:10.1029/2012GL053435.

411 Ezer, T. (2013), Sea level rise, spatially uneven and temporally unsteady: Why the U.S. East Coast, the
412 global tide gauge record, and the global altimeter data show different trends, *Geophys. Res. Lett.*, 40,
413 5439–5444, doi:10.1002/2013GL057952.

414 Ezer, T., L. P. Atkinson, W. B. Corlett and J. L. Blanco (2013), Gulf Stream's induced sea level rise and
415 variability along the U.S. mid-Atlantic coast, *J. Geophys. Res.*, 118, 685–697, doi:10.1002/jgrc.20091.

416 Haigh, I. D., T. Wahl, E. J. Rohling, R. M. Price, C. B. Battiaratchi, F. M. Calafat and S. Dangendorf
417 (2014), Timescales for detecting a significant acceleration in sea level rise. *Nature Communications*,
418 doi:10.1038/ncomms4635.

419 Hakkinen, S. and P. B. Rhines (2004), Decline of subpolar North Atlantic circulation during the 1990s,
420 *Science*, 304, 555-559.

421 Hunter, J. (2010), Estimating sea-level extremes under conditions of uncertain sea-level rise. *Clim.*
422 *Change*, 99, 331-350, doi:10.1007/s10584-009-9671-6.

423 Hunter, J. (2012), A simple technique for estimating an allowance for uncertain sea-level rise. *Clim.*
424 *Change*, 113, 239-252, doi:10.1007/s10584-011-0332-1.

425 Hurrell, J. W. (1995). Decadal trends in the North Atlantic oscillation. *Science*, 269, 676-679.

426 Kemp, A. C. and B. Horton (2013), Contribution of relative sea-level rise to historical hurricane
427 flooding in New York City. *J. Quat. Sci.*, 28(6), 537-541, doi:10.1002/jqs.2653.

428 Kleinosky, L. R., B. Yarnal and A. Fisher (2007), Vulnerability of Hampton Roads, Virginia to storm-
429 surge flooding and sea-level rise. *Nat. Haz.*, 40(1), 43-70, doi: 10.1007/s11069-006-0004-z.

430 Kopp, R. E. (2013), Does the mid-Atlantic United States sea-level acceleration hot spot reflect ocean
431 dynamic variability?. *Geophys. Res. Lett.*, doi:10.1002/grl.50781.

432 Levermann, A., A. Griesel, M. Hofmann, M. Montoya and S. Rahmstorf (2005), Dynamic sea level
433 changes following changes in the thermohaline circulation, *Clim. Dyn.*, 24(4), 347-354.

434 McCarthy, G., E. Frejka-Williams, W. E. Johns, M. O. Baringer, C. S. Meinen, H. L. Bryden, D.
435 Rayner, A. Duche, C. Roberts and S. A. Cunningham (2012), Observed interannual variability of the
436 Atlantic Meridional Overturning Circulation at 26.5°N. *Geophys. Res. Lett.*, DOI:
437 10.1029/2012GL052933.

438 Mills, K. E., A. J. Pershing, C. J. Brown, Y. Chen, F.-S. Chiang, D. S. Holland, S. Lehuta, J. A. Nye, J.
439 C. Sun, T. C. Andrew and R. A. Wahle (2013), Fisheries Management in a Changing Climate
440 Lessons from the 2012 Ocean Heat Wave in the Northwest Atlantic. *Oceanography* 26(2), 191-195.

441 Mitchell, M., C. Hershner, J. Herman, D. Schatt, E. Eggington, and S. Stiles (2013), *Recurrent flooding*
442 *study for Tidewater Virginia*, Report SJR 76, 2012, Virginia Institute of Marine Science, Gloucester
443 Point, VA, pp. 141.

444 Nicholls, R. J., and A. Cazenave, (2010). Sea-level rise and its impact on coastal zones. *Science*,
445 328(5985), 1517-1520.

446 Rossby, T., C. N. Flagg, K. Donohue, A. Sanchez-Franks, and J. Lillibridge (2014), On the long-term
447 stability of Gulf Stream transport based on 20 years of direct measurements, *Geophys. Res. Lett.*, 41,
448 114–120, doi:10.1002/2013GL058636.

449 Sallenger, A. H., K. S. Doran and P. Howd (2012), Hotspot of accelerated sea-level rise on the Atlantic
450 coast of North America, *Nature Clim. Change*, 24 June, doi:10.1038/NCILMATE1597.

451 Smeed, D. A., G. McCarthy, S. A. Cunningham, E. Frajka-Williams, D. Rayner, W. E. Johns, C. S.
452 Meinen, M. O Baringer, B. I. Moat, A. Duche and H. L. Bryden (2013), Observed decline of the
453 Atlantic Meridional Overturning Circulation 2004 to 2012. *Ocean Sci. Discus.* 10, 1619-1645.

454 Srokosz, M., M. Baringer, H. Bryden, S. Cunningham, T. Delworth, S. Lozier, J. Marotzke, and R.
455 Sutton (2012), Past, present, and future changes in the Atlantic meridional overturning circulation.
456 *Bull. Amer. Met. Soc.*, doi:10.1175/BAMS-D-11-00151.1, 1663-1676.

457 Sweet, W., C. Zervas and S. Gill (2009), Elevated east coast sea level anomaly: June-July 2009, NOAA
458 Tech. Rep. No. NOS CO-OPS 051, NOAA National Ocean Service, Silver Spring, MD, 40pp.

459 Yin, J., M. E. Schlesinger, and R. J. Stouffer (2009), Model projections of rapid sea-level rise on the
460 northeast coast of the United States. *Nature Geoscience*, Vol. 2, doi:10.1038/NCEO462, 262-266.

461 Yin, J., and P. B. Goddard (2013), Oceanic control of sea level rise patterns along the East Coast of the
462 United States, *Geophys. Res. Lett.*, 40, 5514–5520, doi:10.1002/2013GL057992.

463 Zervas, C. (2009), Sea level variations of the United States 1854-2006. NOAA Tech. Rep. NOS CO-
464 OPS 053, 78pp, NOAA/National Ocean Service, Silver Spring, MD.

465 Zhang, H., and J. Sheng (2013), Estimation of extreme sea levels over the eastern continental shelf of
466 North America, *J. Geophys. Res. Oceans*, 118, 6253–6273, doi:10.1002/2013JC009160.

467 Zhang, K. (2011), Analysis of non-linear inundation from sea-level rise using LIDAR data: a case study
468 for south Florida. *Clim. Change*, 106, 535-565, doi:10.1007/s10584-010-9987-2.

469 Zhao, J. and W. Johns (2014), Wind-forced interannual variability of the Atlantic Meridional
470 Overturning Circulation at 26.5°N. *J. Geophys. Res. Oceans*, 119, 6253–6273,
471 doi:10.1002/2013JC009407.

472

473 **Table 1.** Information about the hourly sea level data used in this study and the calculated statistics. The
474 mean high tidal range is defined as the difference between MHHW and MLLW. The mean sea level rise
475 (SLR) obtained from linear regression and the 95% confidence interval are estimated based on Zervas
476 (2009). The minor flooding estimate for different periods is based on the hours per year with water level
477 at least 0.3m over MHHW; the 2 stations in the extreme north and south were neglected in the
478 calculations of the mean flooding of all stations (last 4 columns of the bottom row). ACC is the
479 estimated acceleration in flooding time (see Eq. 3 in text).
480

| Station name, location and starting hourly data (all end in 2013) | | | | Sea level statistics | | | | | |
|--|-------------|-------------|--------|----------------------|----------------|---------------------|---------------|---------------|--------------------|
| | | | | Tidal range (m) | SLR (mm/y) | hours/yr of WL>0.3m | | | ACC |
| | Lat (°N) | Lon (°W) | Y1 | MHHW- MLLW | Mean ±95%CI | Y1- 1970 | 1971- 1990 | 1991- 2013 | hr/yr ² |
| 1. Eastport, ME | 44.90 | 66.98 | 1958 | 5.87 | 1.93±0.5 | 127 | 110 | 183 | 0.24 |
| 2. Portland, ME | 43.66 | 70.25 | 1911 | 3.02 | 1.89±0.2 | 38 | 79 | 109 | 0.013 |
| 3. Boston, MA | 42.35 | 71.05 | 1922 | 3.13 | 2.79±0.2 | 40 | 71 | 116 | 0.045 |
| 4. Battery, NY | 40.70 | 74.01 | 1920 | 1.54 | 3.12±0.2 | 19 | 41 | 99 | 0.076 |
| 5. Atlantic City, NJ | 39.36 | 74.42 | 1912 | 1.40 | 4.16±0.2 | 12 | 33 | 94 | 0.078 |
| 6. Lewes, DE | 38.78 | 75.12 | 1967 | 1.42 | 3.82±0.7 | 31 | 33 | 89 | 0.150 |
| 7. Norfolk, VA | 36.95 | 76.33 | 1927 | 0.84 | 4.54±0.2 | 19 | 39 | 128 | 0.136 |
| 8. Wilmington, NC | 34.23 | 77.95 | 1938 | 1.43 | 2.01±0.3 | 2.5 | 6 | 28 | 0.038 |
| 9. Charleston, SC | 32.78 | 79.93 | 1922 | 1.76 | 3.15±0.2 | 12 | 27 | 71 | 0.060 |
| 10. Ft. Pulaski, GA | 32.03 | 80.90 | 1921 | 2.29 | 3.16±0.2 | 19 | 41 | 99 | 0.076 |
| 11. Key West, FL | 24.56 | 81.81 | 1913 | 0.55 | 2.39±0.2 | 4 | 4.5 | 13 | 0.013 |
| mean± SD | | | 87 yrs | 1.92±0.8 | 3.00±0.9 | 21±13 | 41±22 | 92±29 | |

481

482

483
484 **Figure Captions**
485 **Figure 1.** Map of the U.S. East Coast (based on Google Earth) and location of tide gauge stations.
486
487 **Figure 2.** Comparison of monthly sea level in Norfolk (green) with global mean sea level obtained from
488 tide gauges (blue) and AVISO satellite altimeters (red). The different contributions to a storm surge
489 event are illustrated. See *Ezer* [2013] for information on the global data sets.
490
491 **Figure 3.** Maximum measured water level (relative to MHHW, defined by the mean of the epoch
492 period 1982-2001) at Sewells Point, Norfolk, VA, during the top 17 storm surges . The sea level rise
493 during the observed period is indicated by the blue line. . The total amplitude of the storm surge relative
494 to the mean water level at the time of the storm is the difference between the top of the green bar and the
495 blue line.
496
497 **Figure 4a.** Potential flooding statistics for Eastport, ME, in the Gulf of Maine. From bottom to top: 1)
498 hourly sea level data, and hours per year of water reaching 2) 0.3 m, 3) 0.6 m and 4) 0.9 m above
499 MHHW (the values in meter are exact while the values in feet are approximated; the Imperial/U.S.
500 Customary Units are listed since they are used in weather reports and flood risk assessment in the U.S.).
501 Yellow, white and red lines in 1) indicate linear SLR trend, MHHW, and the 3 flood lines, respectively.
502
503 **Figure 4b.** Same as Fig. 4a, but for Portland, ME, in the Gulf of Maine.
504
505 **Figure 4c.** Same as Fig. 4a, but for Battery station, New York, NY.
506
507 **Figure 4d.** Same as Fig. 4a, but for Sewells Point, Norfolk, VA, in the lower Chesapeake Bay.
508
509 **Figure 4e.** Same as Fig. 4a, but for Wilmington, NC. The station is located in the Cape Fear River,
510 which is connected to the South-Atlantic Bight.
511
512 **Figure 4f.** Same as Fig. 4a, but for Charleston, SC, in the South-Atlantic Bight.
513
514 **Figure 4g.** Same as Fig. 4a, but for Key West, FL.
515
516 **Figure 5.** Summary of the mean number of hours per year of water level of at least 0.3 m above
517 MHHW. Green, blue and red bars are averages over 3 different periods, before 1971, 1971-1990, and
518 after 1991-2013, respectively. The percentage increase in potential minor flooding from the first to the
519 third period is indicated for each station.
520
521
522 **Figure 6.** Acceleration in SLR [in mm y^{-2} , from *Ezer*, 2013] versus acceleration in minor flooding (in
523 annual flood hours of 0.3m over MHHW per year per year); see text for details of the calculations. The
524 data from Eastport is omitted due to its unusual high tide relative to other stations (Fig. 5). The linear
525 regression line (in green), the correlation coefficient and the confidence level of the correlation are
526 indicated.
527

528 **Figure 7.** The impact of tidal range on potential minor flooding (0.3 m above MHHW). The green, blue
529 and red markers and line fit represent the same 3 periods as in Fig. 5. The linear correlation coefficients
530 and statistical confidence level are indicated.

531
532 **Figure 8.** The number of extreme storm surge events versus the North Atlantic Oscillation (NAO)
533 Index. Green line and axis on the right: index of “high-water storm events” calculated by the average
534 number of storm surges per year in for each 5-year period. A storm event is defined as a year in which
535 water level reached 0.9 m over MHHW at least once at any station (i.e., each non-zero bar in the top
536 panels of figures 4a-4e is considered as a “storm event”). Multiple storms hitting the same location on
537 the same year is counted once, but impact of same storm at 2 different locations is considered as 2
538 impacts. Blue line and axis on the left: 5-year averaged NAO index. Each marker is located at the
539 beginning of a 5-year period. The vertical red dash lines indicate times where high/low peaks in storm
540 events coincide with low/high peaks in the NAO Index.

541 **Figure 9.** (a) Example of hourly water level in Sewells Point, Norfolk, from January to March, 2013.
542 Red, blue and green lines represent observed water level, tidal prediction and residual (observed-
543 prediction), respectively. (b) Daily Florida Current (FC) transport recorded by the cable data across the
544 Florida Straits. (c) The water level residual anomaly in Norfolk (green; in cm) and the FC transport
545 change (blue; in Sv change per day times $10 = 10^5 \text{ m}^3 \text{ d}^{-1}$); the correlation coefficient and confidence
546 level of the correlation between sea level anomaly and FC change are indicated.

547



Eastport

Portland

Boston

Gulf of Maine

New York

Lewes

Mid-Atlantic Bight

Norfolk

Cape Hatteras

Atlantic Ocean

Wilmington

Charleston

Pulaski

South-Atlantic Bight

Fig.1

Key West

Data SIO, NOAA, U.S. Navy, NGA, GEBCO
Image Landsat

Observed Monthly Sea Level

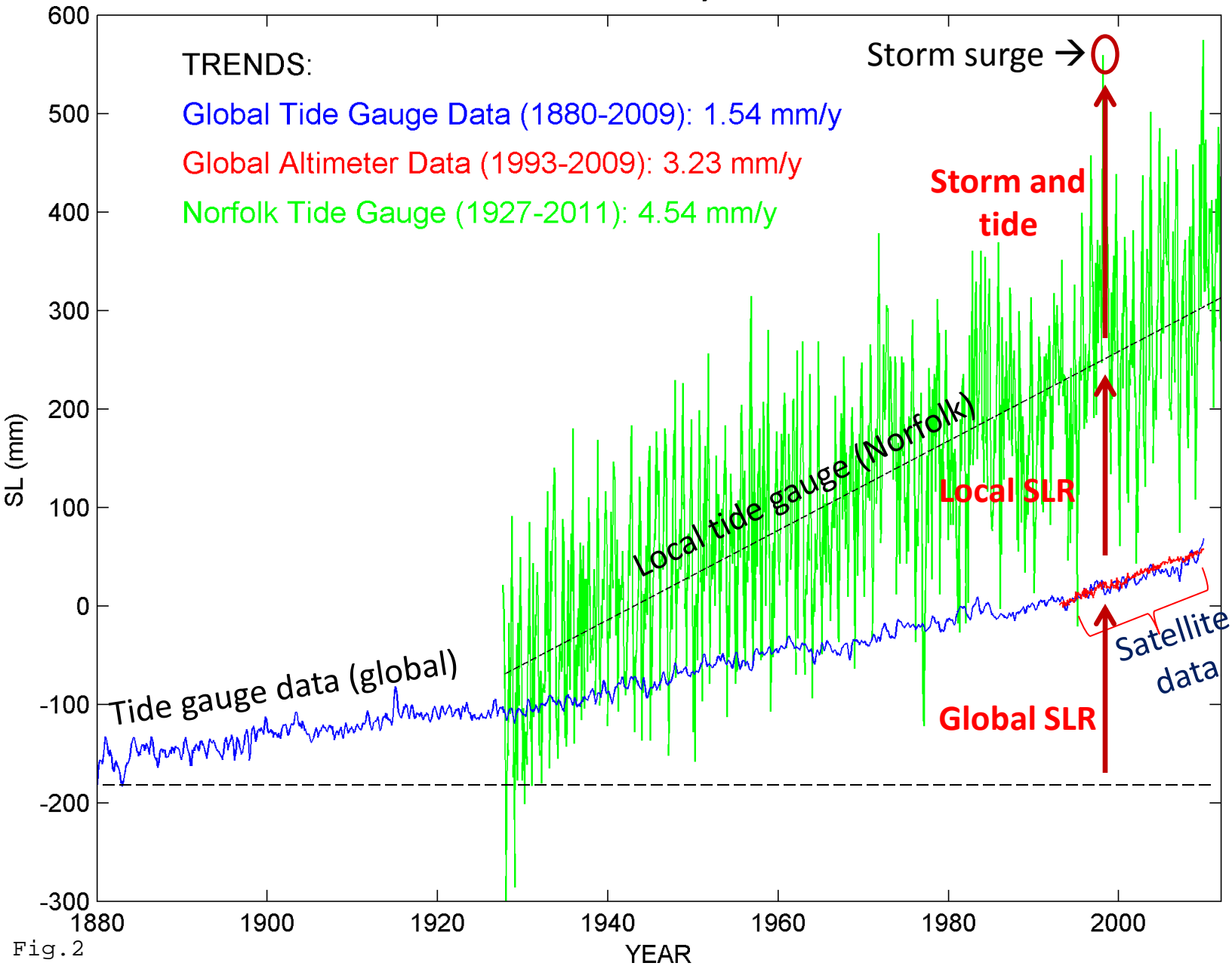


Fig.2

Top Storm Surges in Norfolk

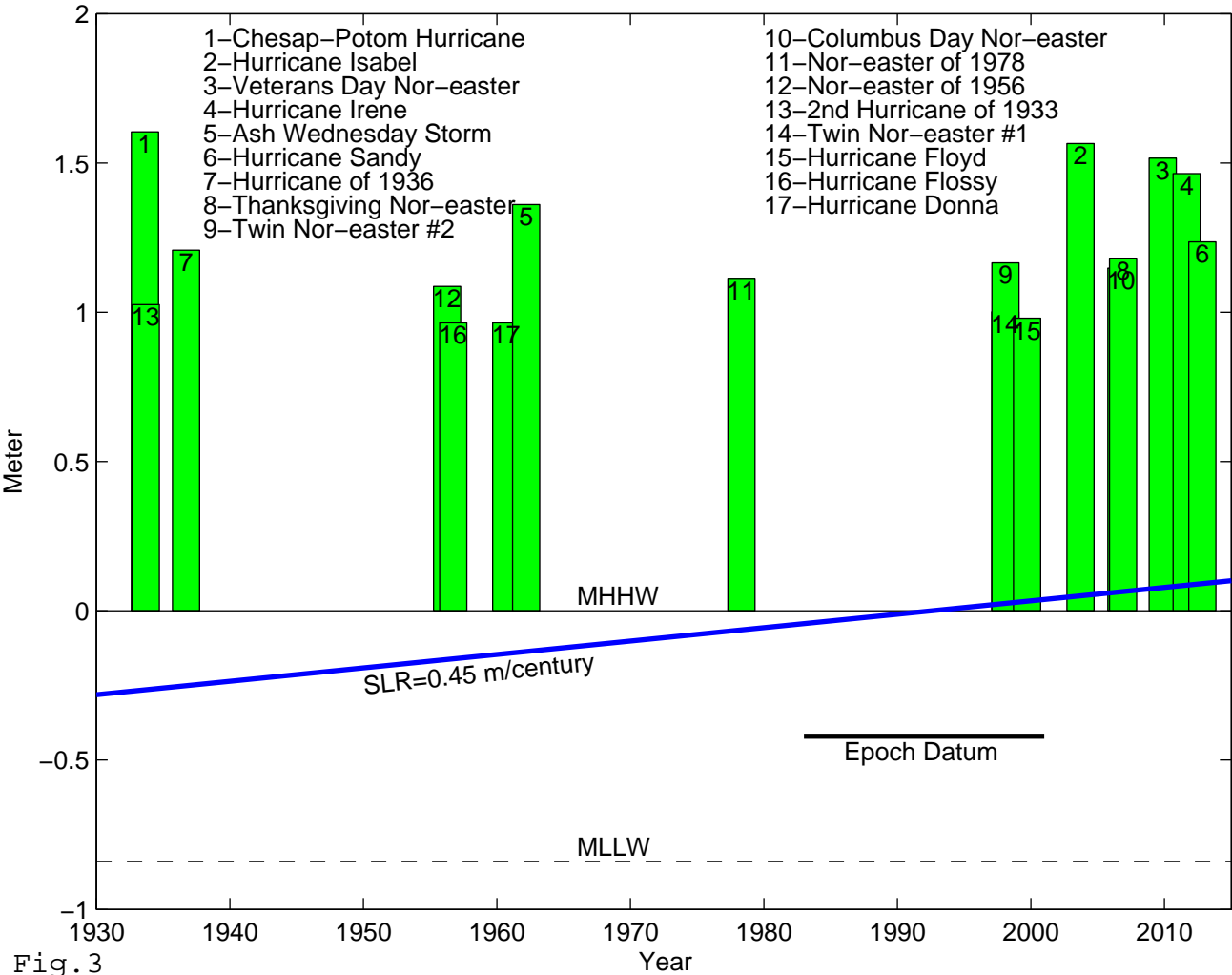
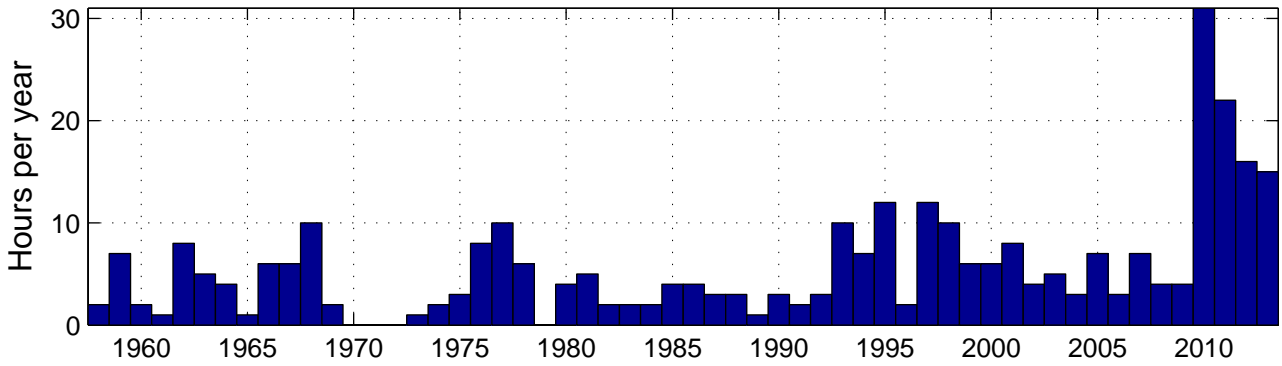
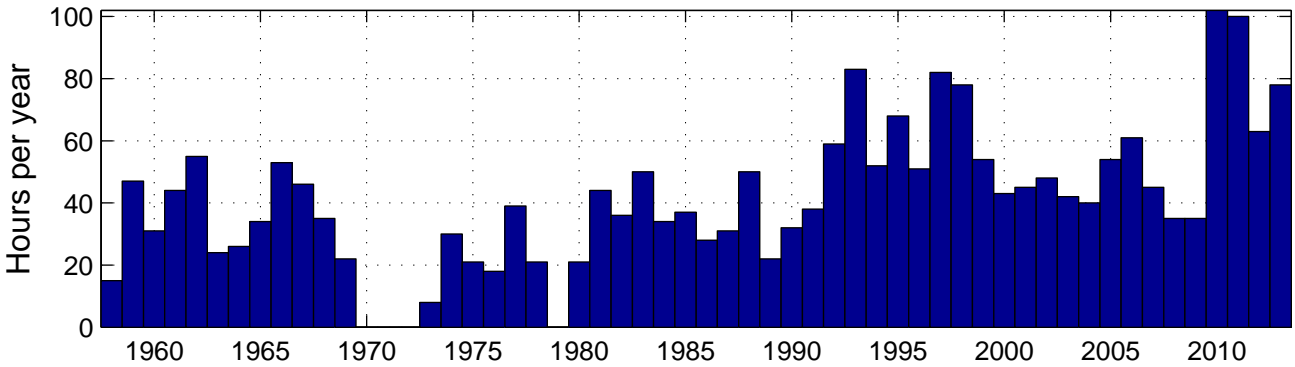


Fig. 3

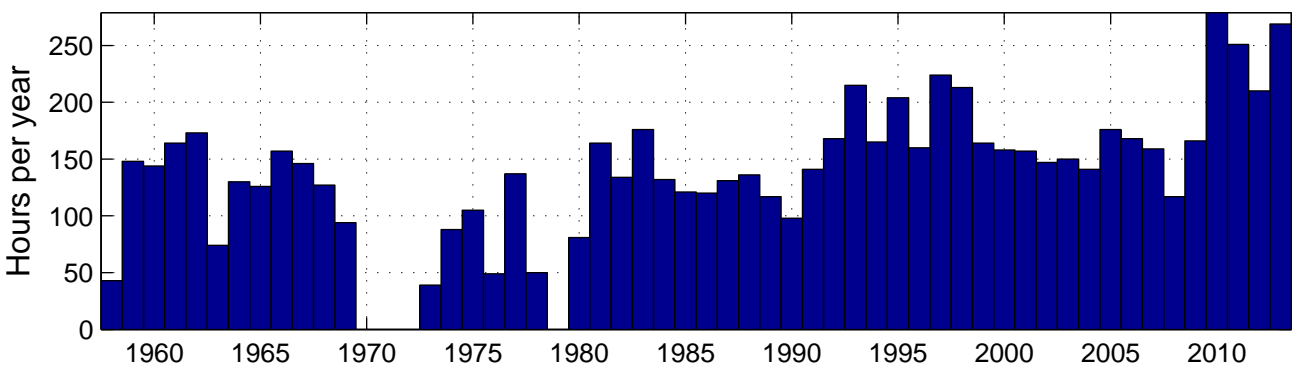
Hours per year 3ft (0.9m) above MHHW in Eastport



Hours per year 2ft (0.6m) above MHHW in Eastport



Hours per year 1ft (0.3m) above MHHW in Eastport



Hourly sea level data in Eastport

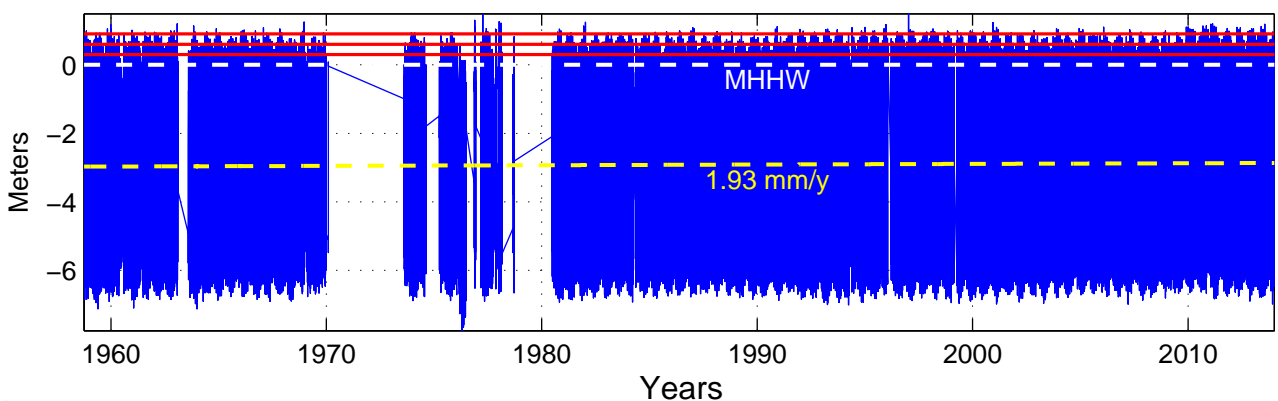
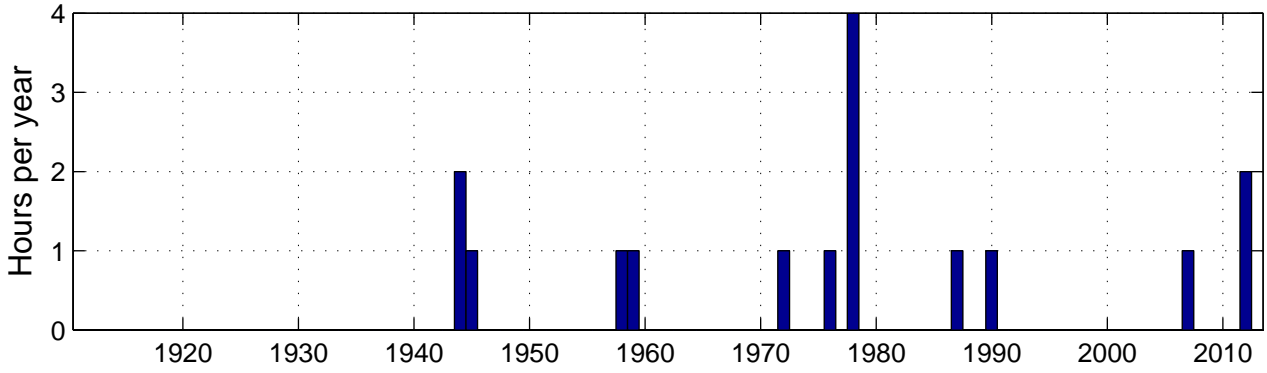
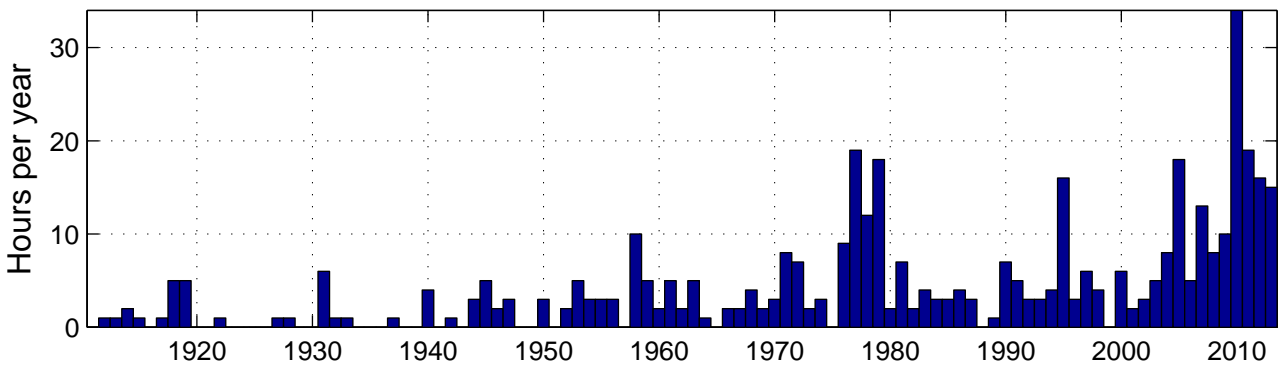


Fig. 4a

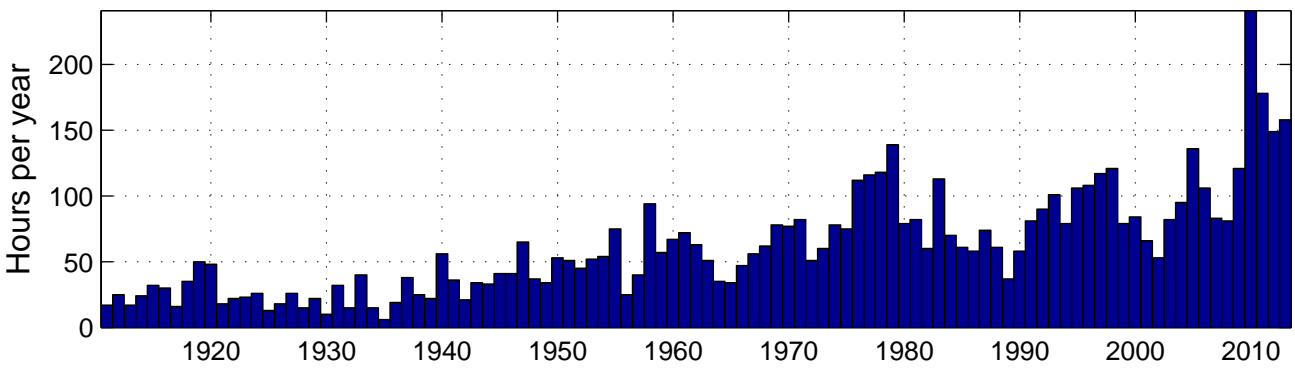
Hours per year 3ft (0.9m) above MHHW in Portland



Hours per year 2ft (0.6m) above MHHW in Portland



Hours per year 1ft (0.3m) above MHHW in Portland



Hourly sea level data in Portland

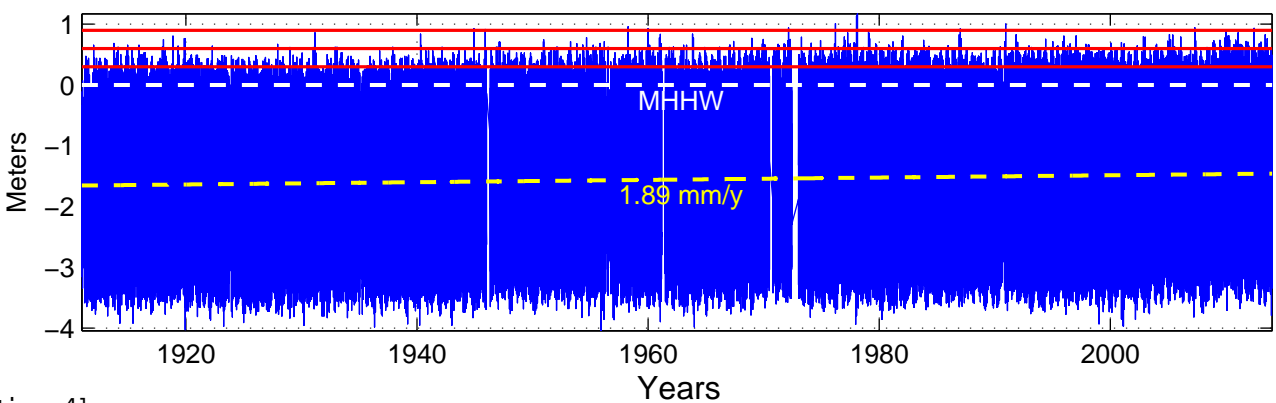
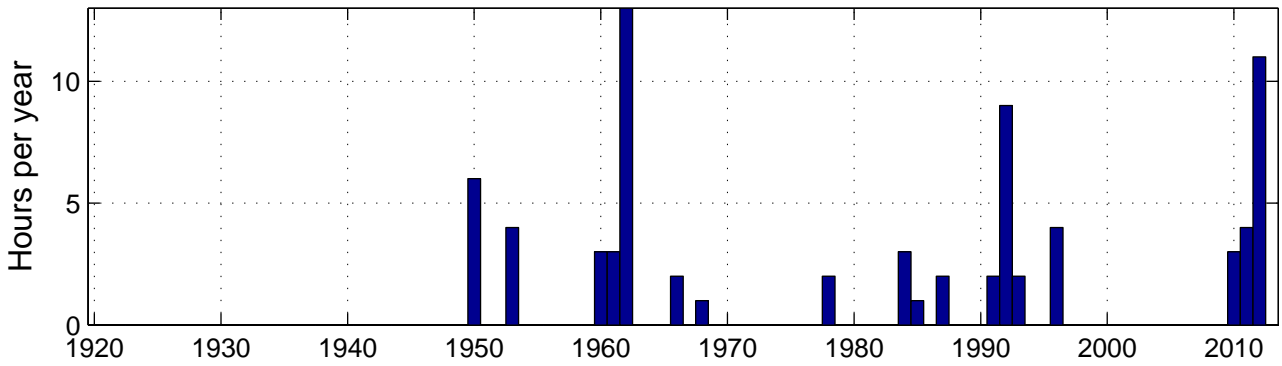
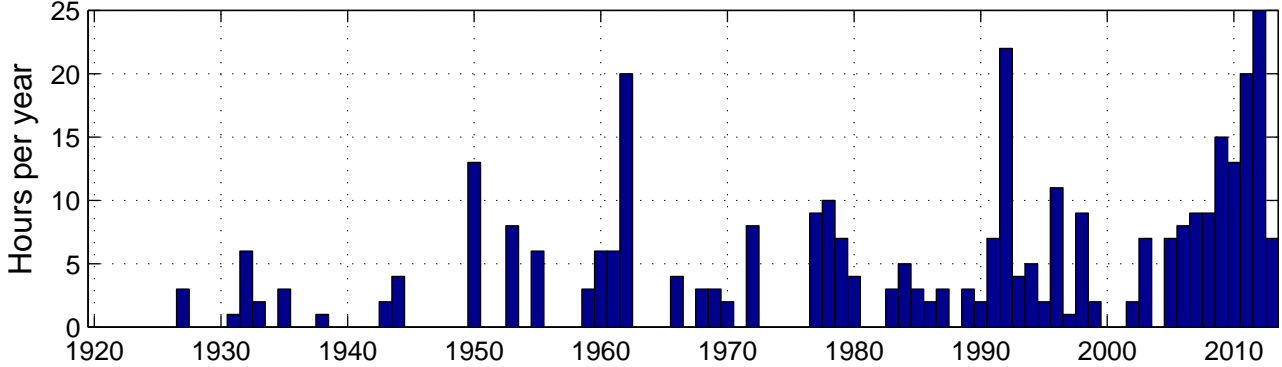


Fig.4b

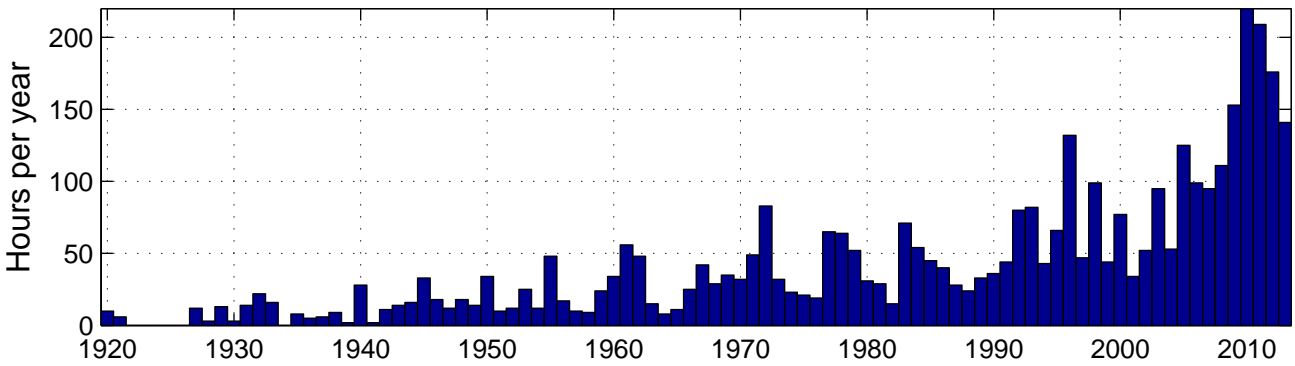
Hours per year 3ft (0.9m) above MHHW in New York



Hours per year 2ft (0.6m) above MHHW in New York



Hours per year 1ft (0.3m) above MHHW in New York



Hourly sea level data in New York

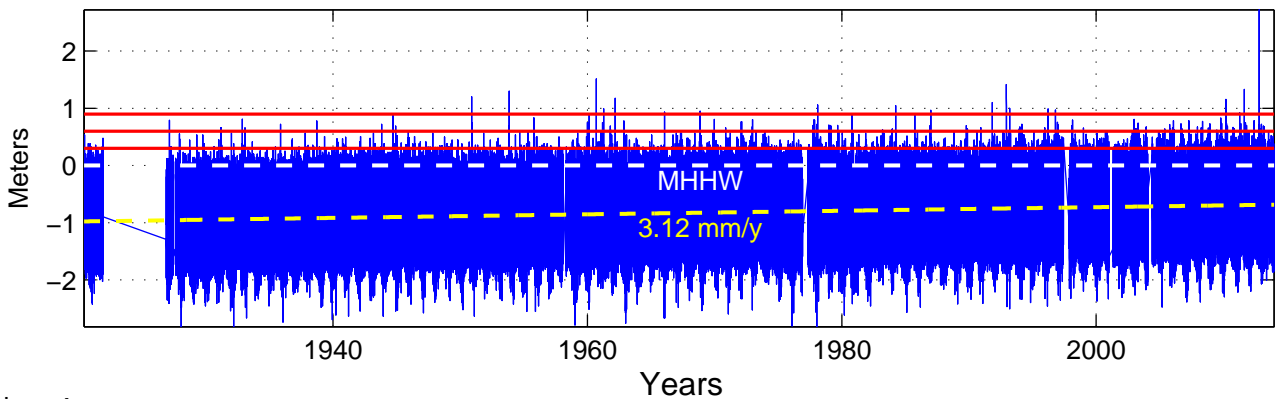
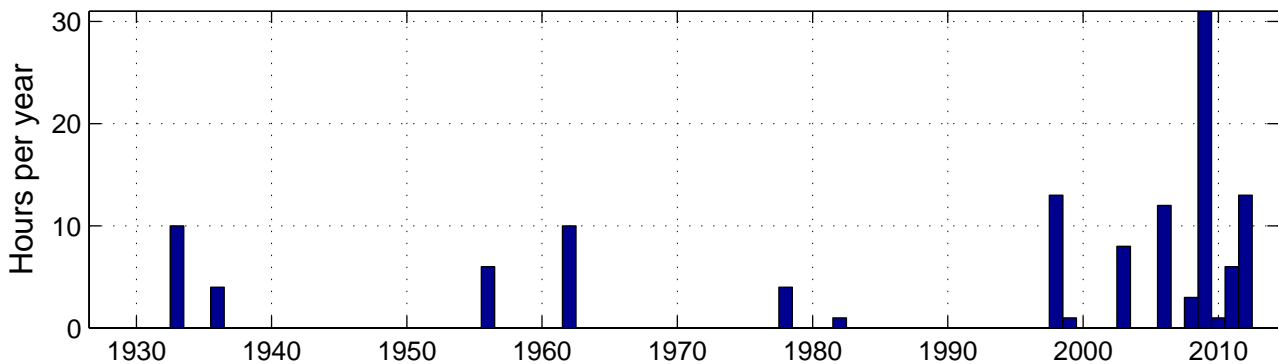
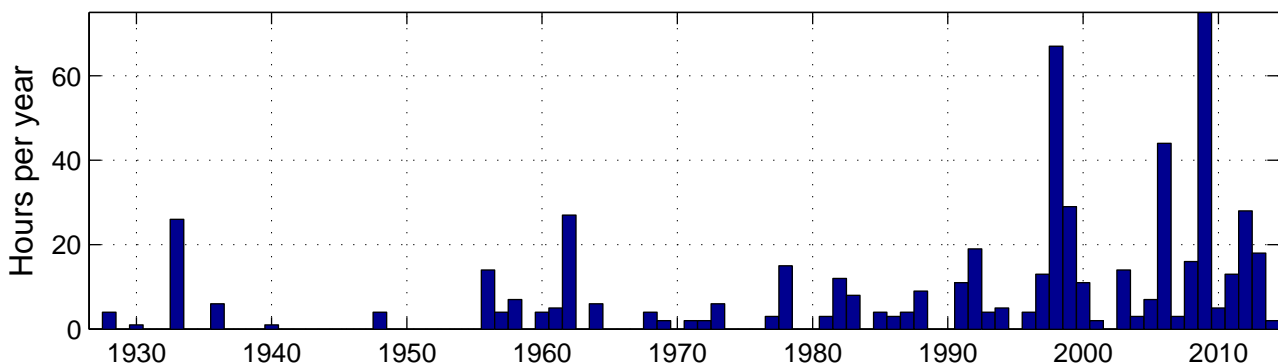


Fig. 4c

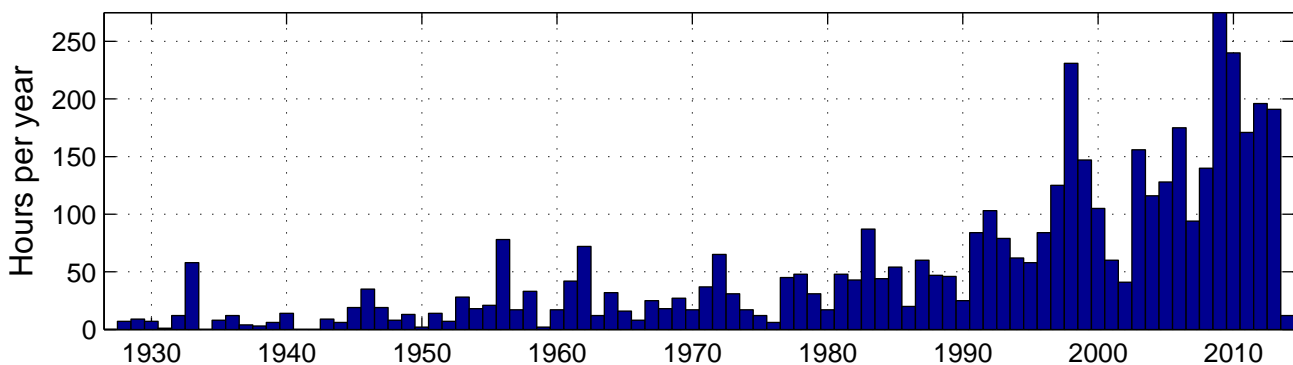
Hours per year 3ft (0.9m) above MHHW in Norfolk



Hours per year 2ft (0.6m) above MHHW in Norfolk



Hours per year 1ft (0.3m) above MHHW in Norfolk



Hourly sea level data in Norfolk

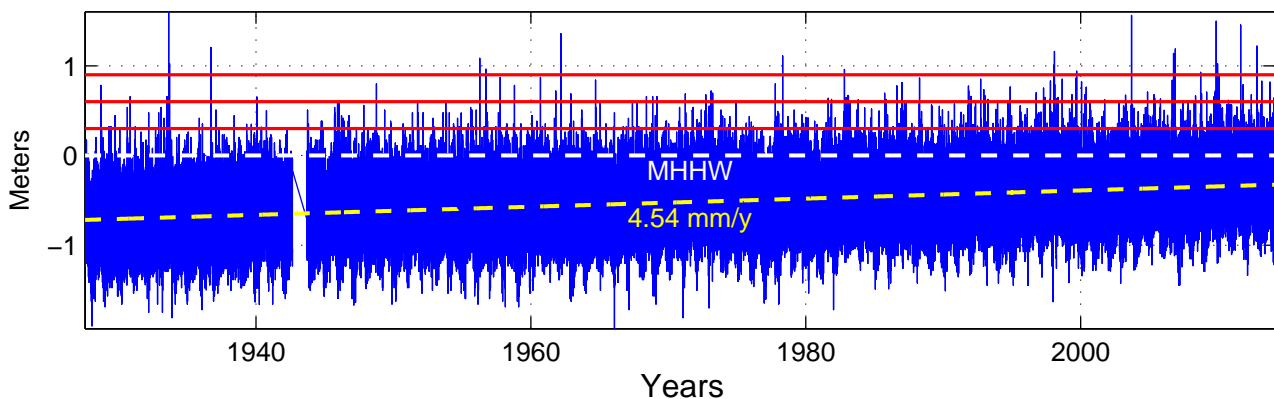
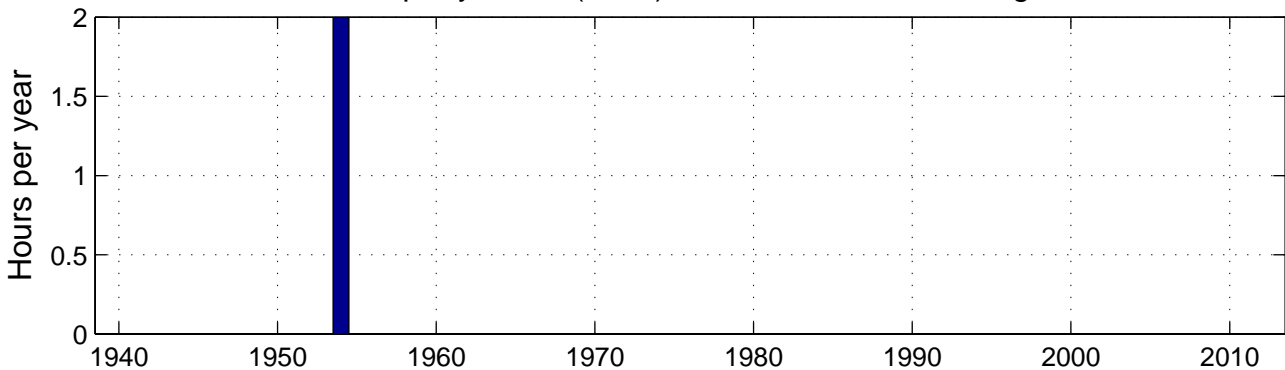
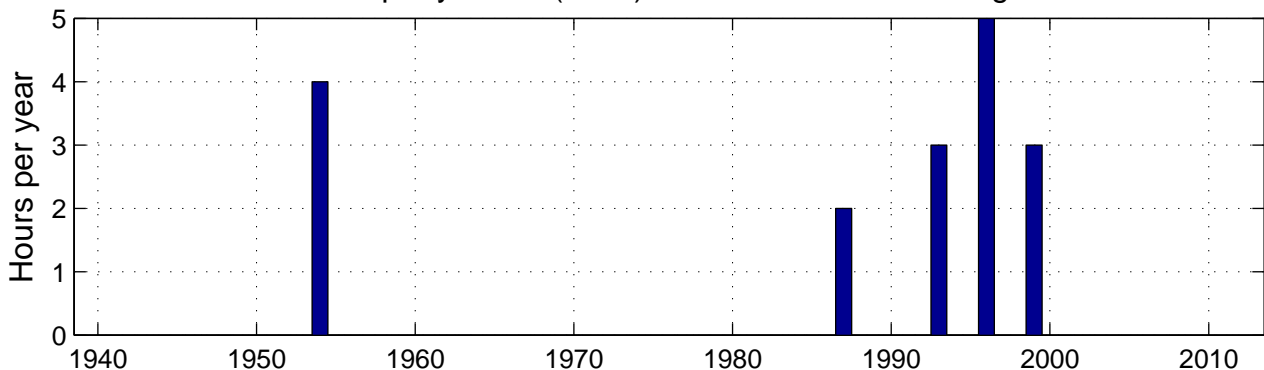


Fig. 4d

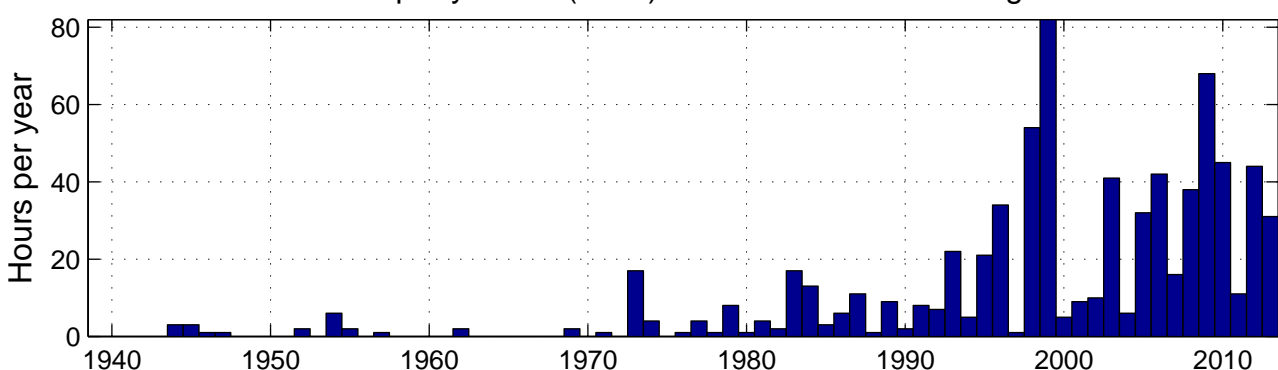
Hours per year 3ft (0.9m) above MHHW in Wilmington



Hours per year 2ft (0.6m) above MHHW in Wilmington



Hours per year 1ft (0.3m) above MHHW in Wilmington



Hourly sea level data in Wilmington

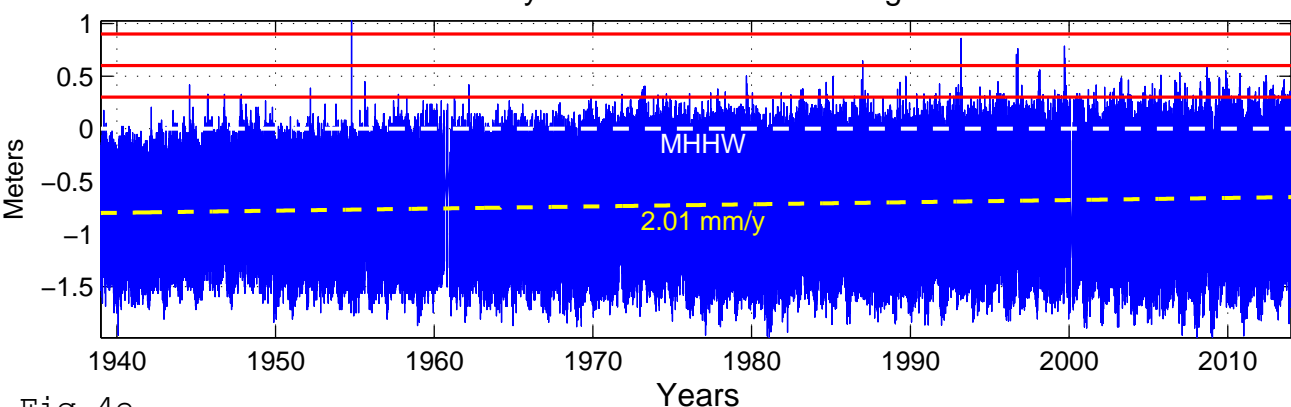
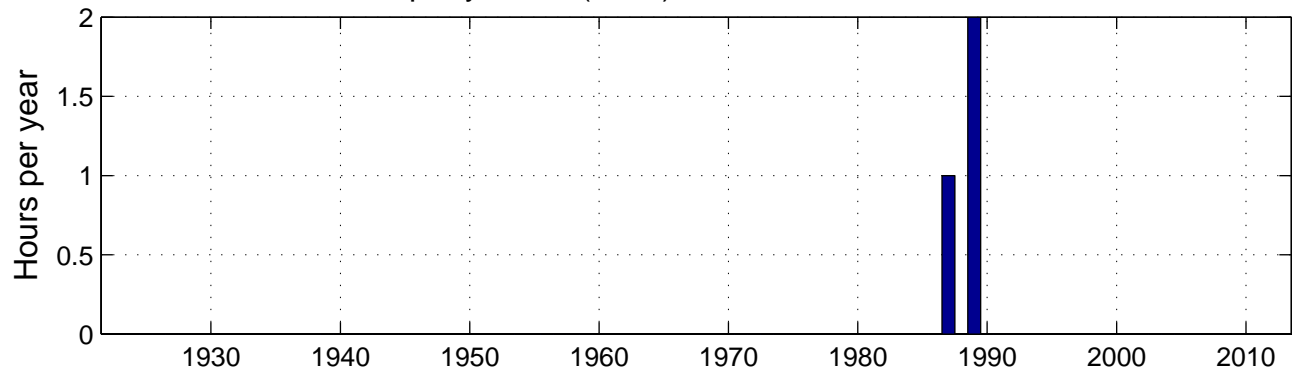
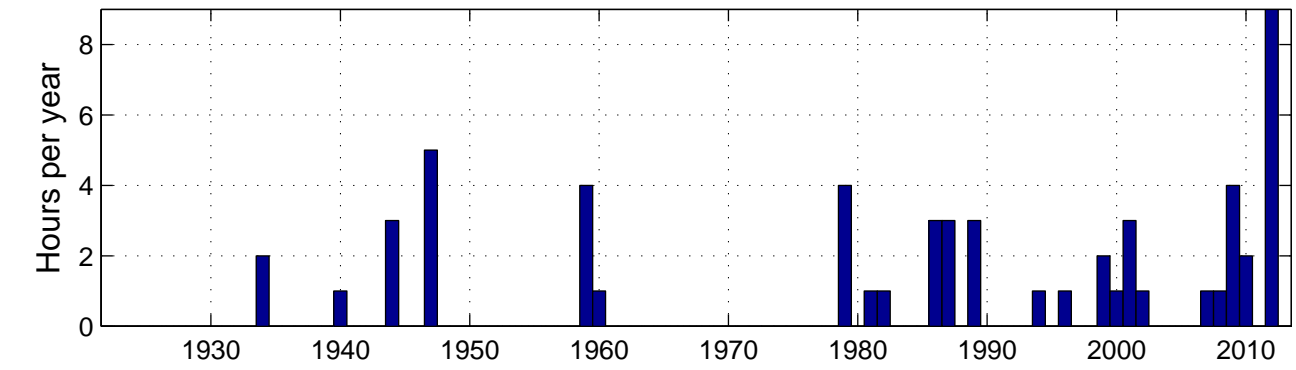


Fig. 4e

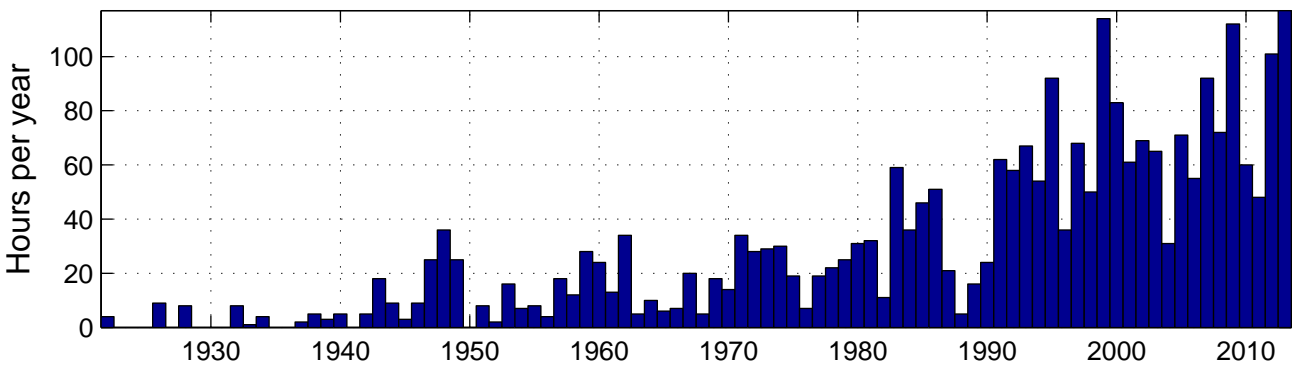
Hours per year 3ft (0.9m) above MHHW in Charleston



Hours per year 2ft (0.6m) above MHHW in Charleston



Hours per year 1ft (0.3m) above MHHW in Charleston



Hourly sea level data in Charleston

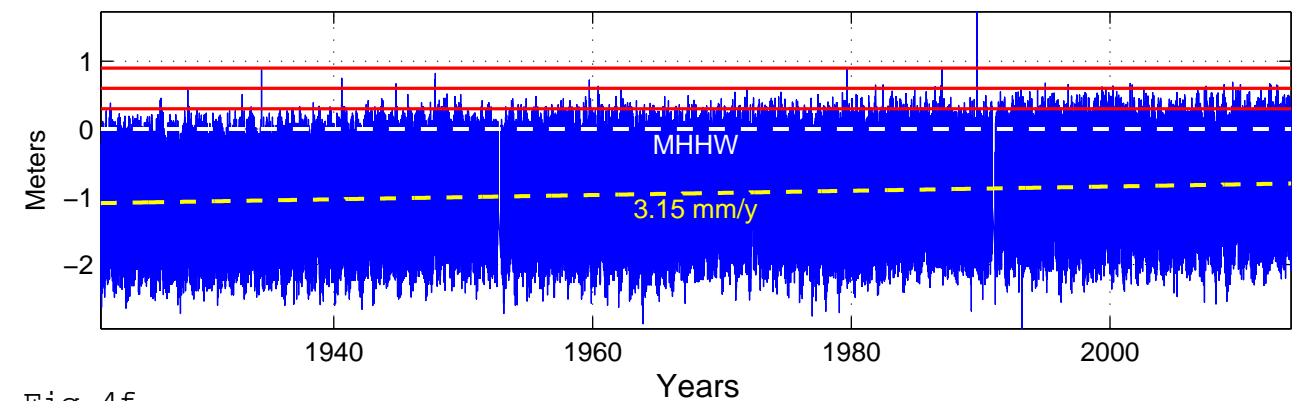
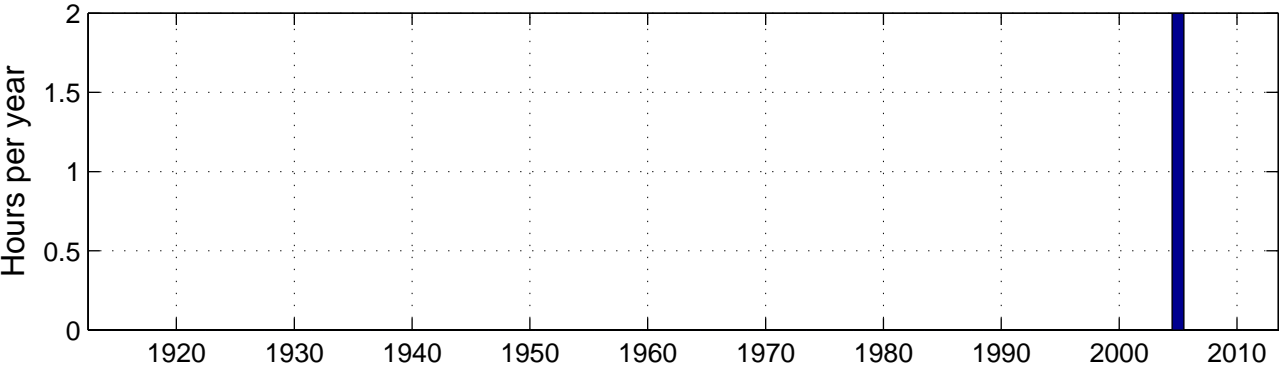
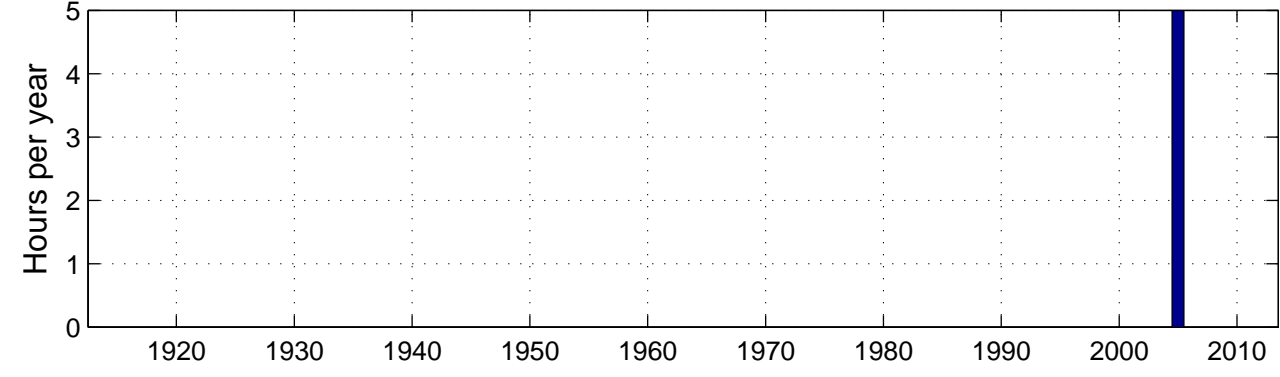


Fig. 4f

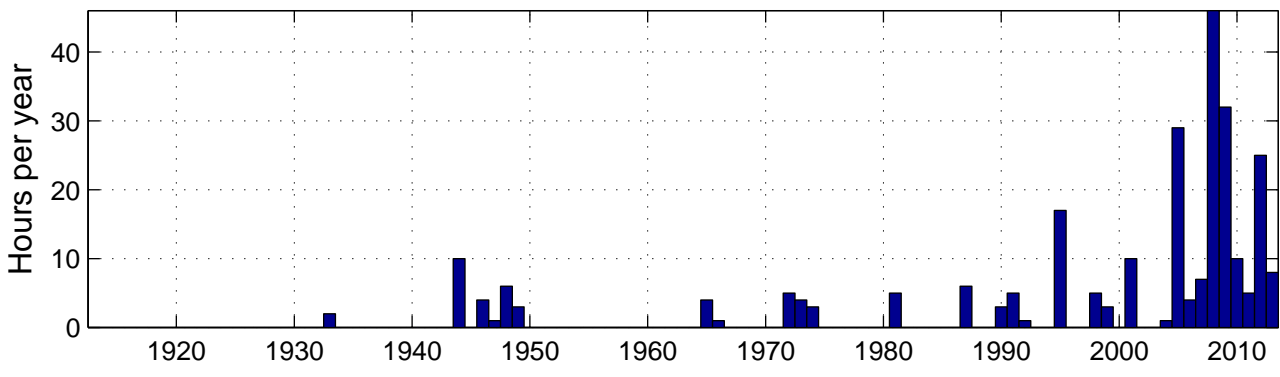
Hours per year 3ft (0.9m) above MHHW in KeyWest



Hours per year 2ft (0.6m) above MHHW in KeyWest



Hours per year 1ft (0.3m) above MHHW in KeyWest



Hourly sea level data in KeyWest

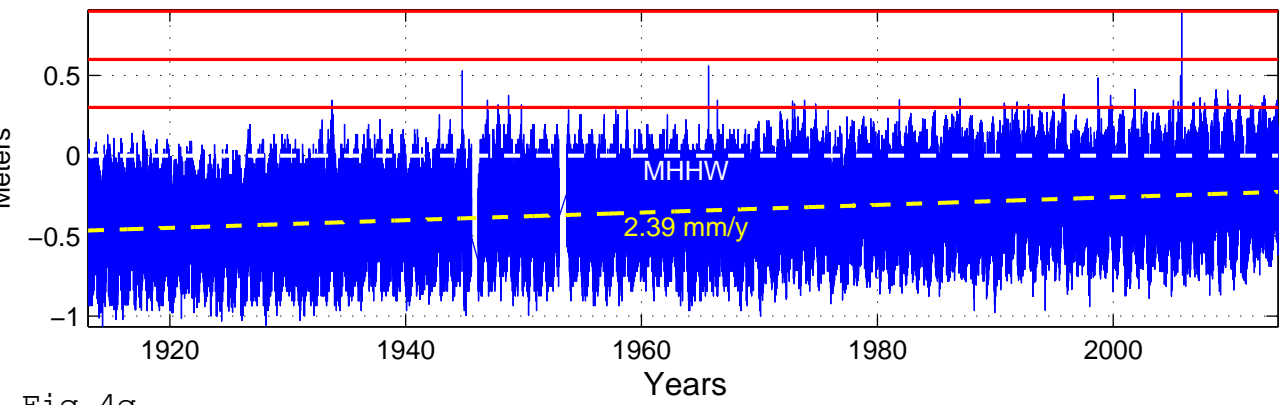


Fig. 4g

Hours/year with sea level at least 0.3m above MHHW

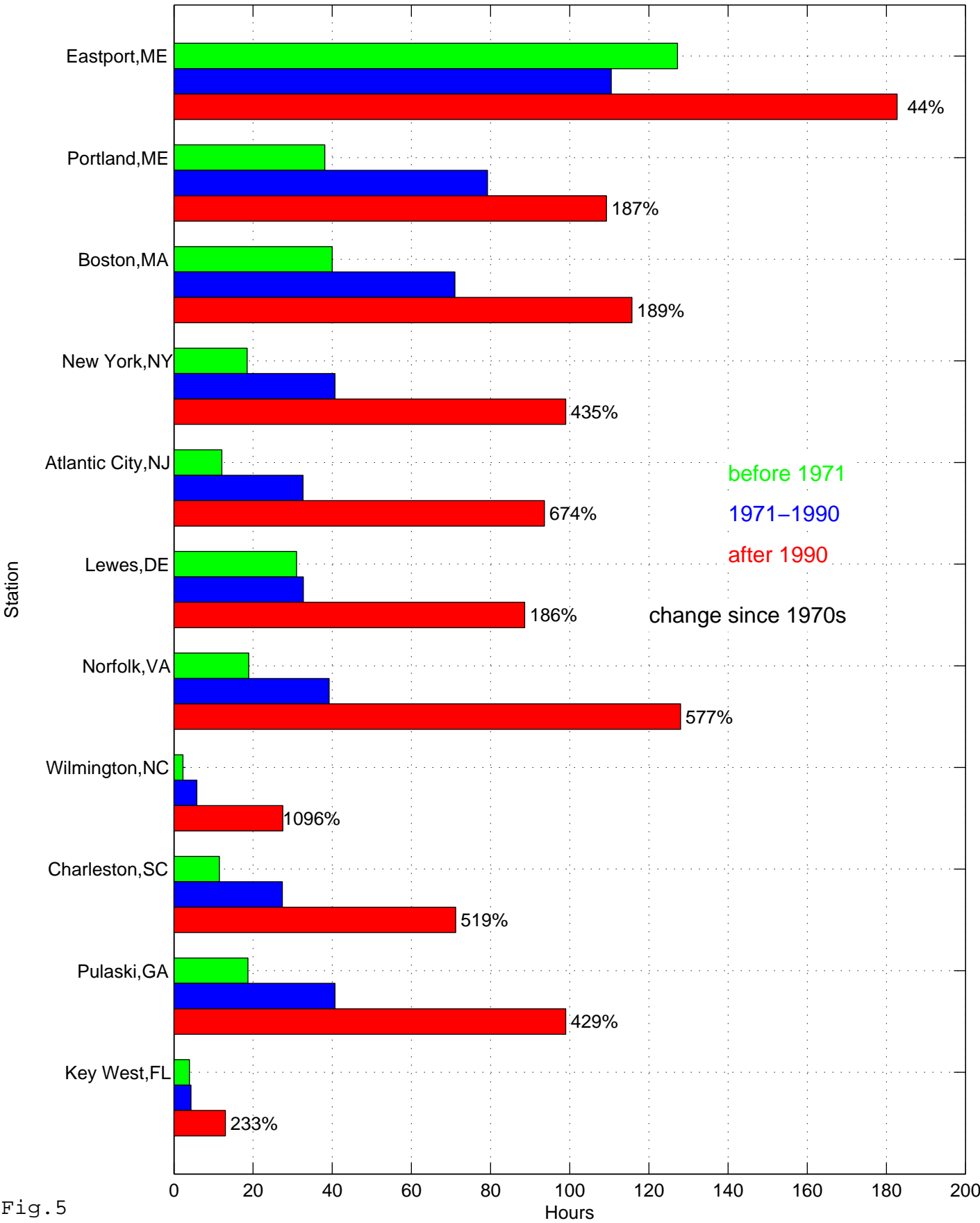


Fig.5

Acceleration of Sea Level vs. Acceleration of Minor Flood Hours

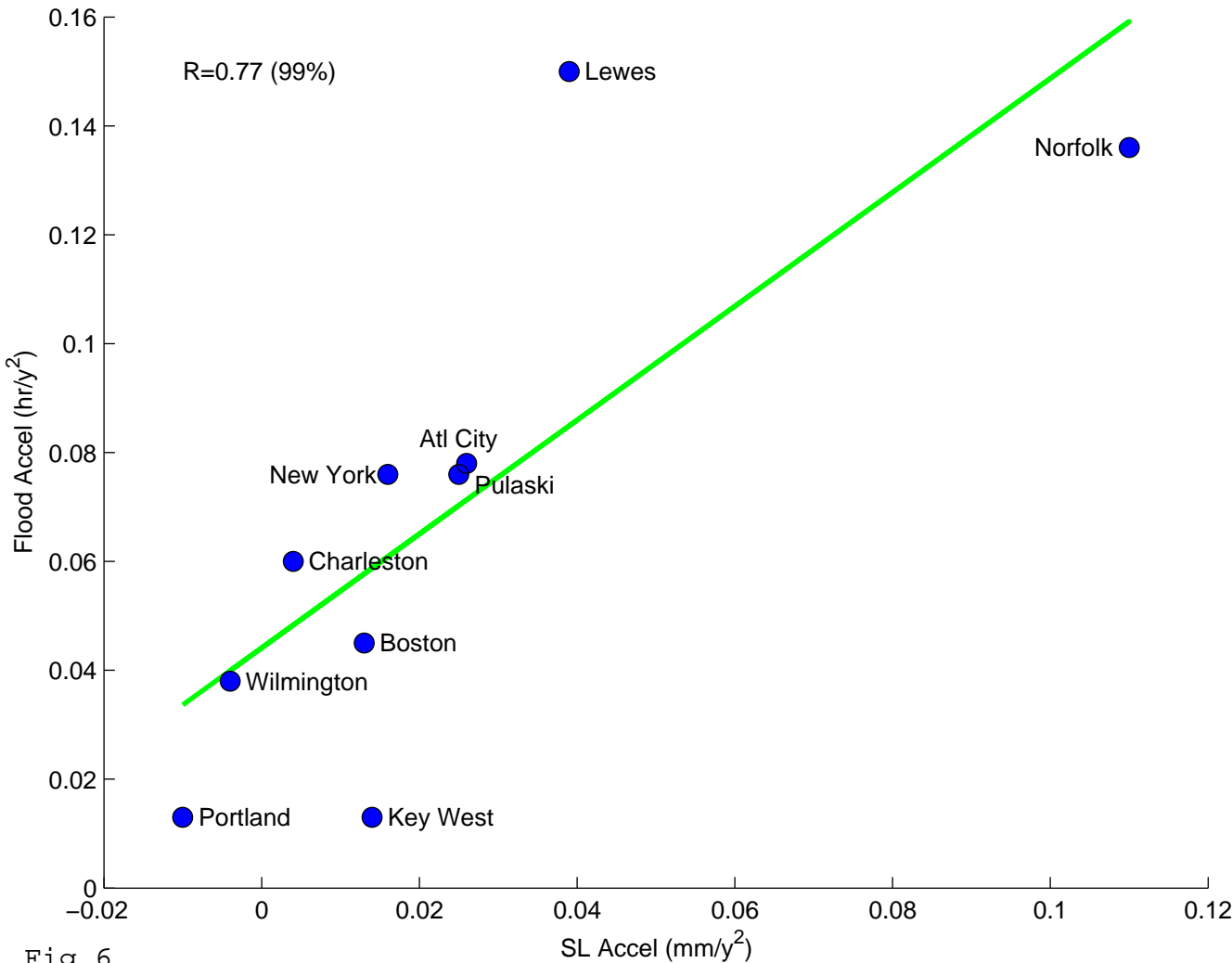


Fig. 6

Tidal range vs. hours of minor flooding

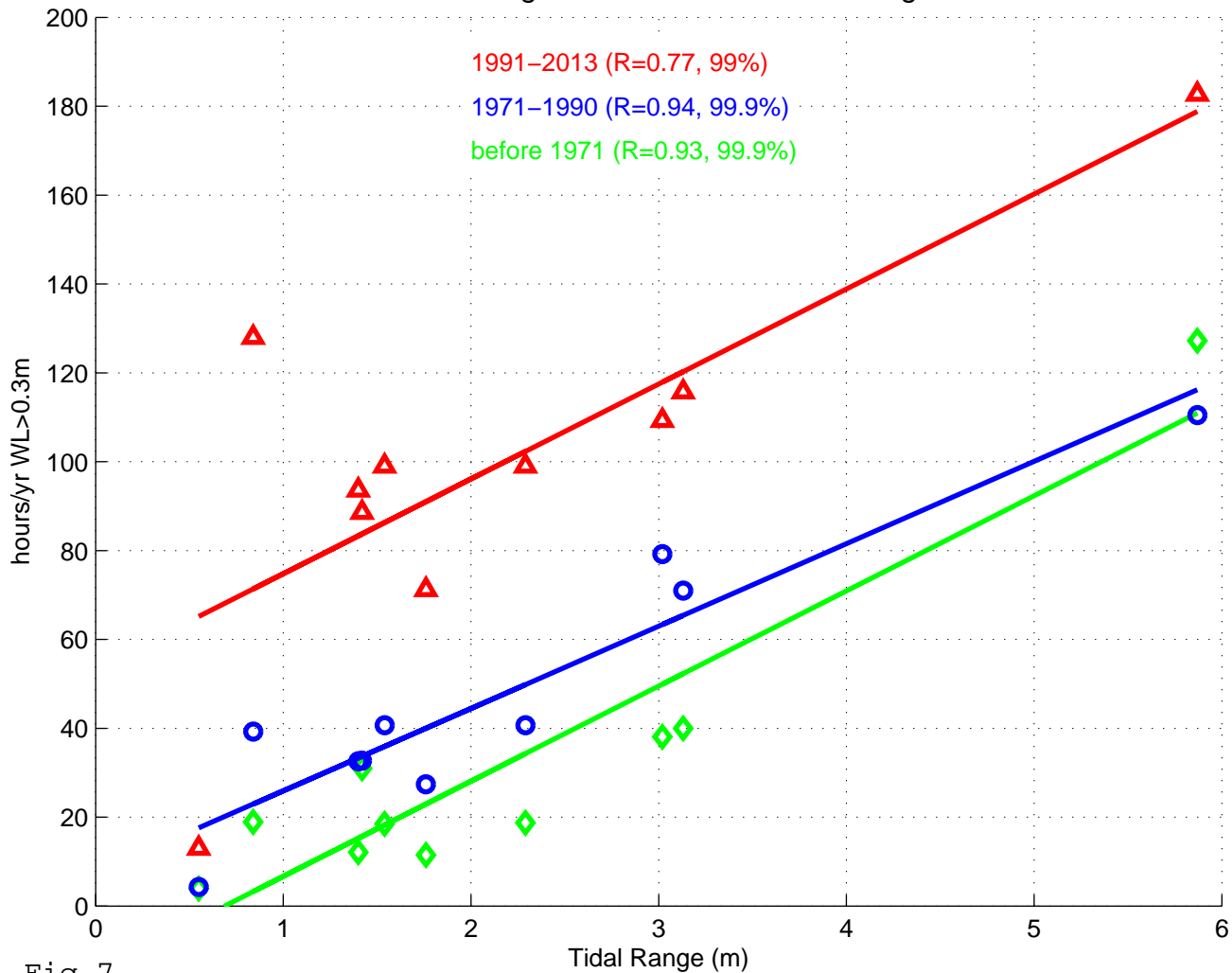


Fig. 7

NAO Index vs. Number of Storms (WL>0.9m)

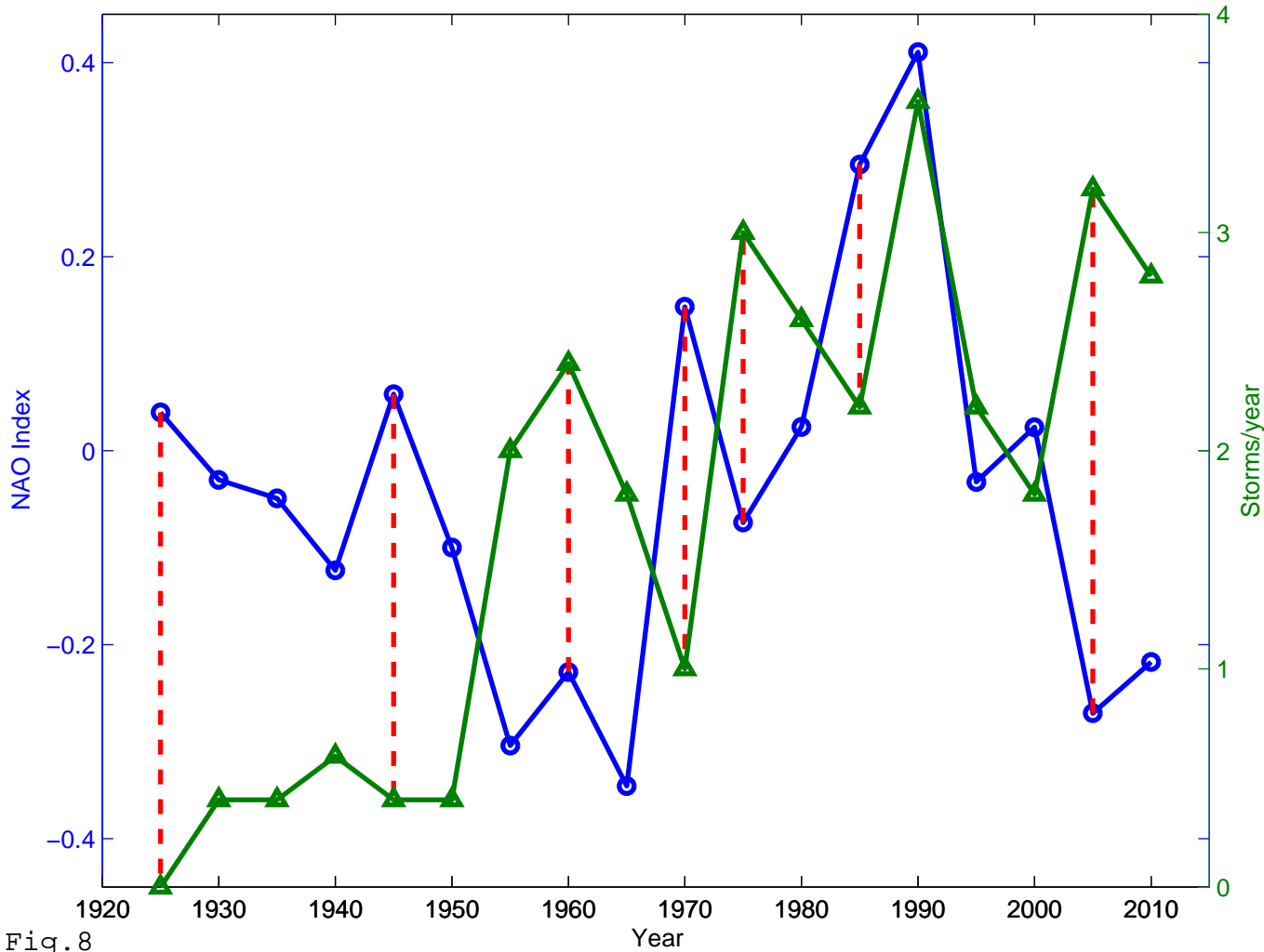
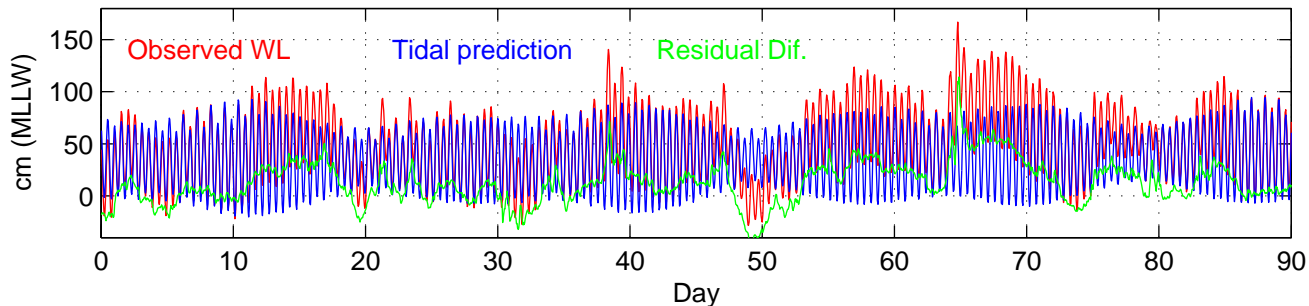
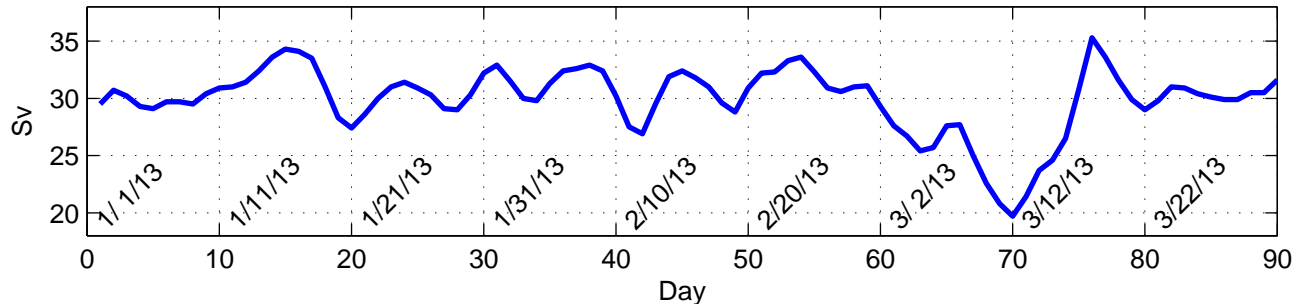


Fig. 8

(a) Hourly Water Level in Norfolk (Jan–Mar, 2013)



(b) Florida Current Daily Transport (Jan–Mar, 2013)



(c) Florida Current Transport Change vs. Residual Sea Level

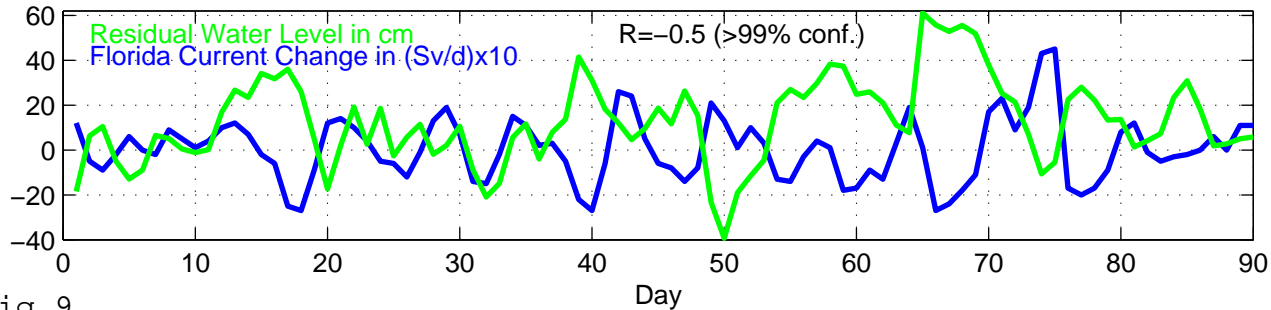


Fig. 9